Mountain Pine Beetle Outbreaks in Western Canada:
Coupled Influences of Climate Variability and Stand Development

Final Report for Climate Change Action Fund Project A676

23 June 2005

R.D. (Dan) Moore (Principal Investigator)

I.G. McKendry

Kerstin Stahl

Department of Geography

The University of British Columbia

H.P. Kimmins

Yueh-Hsien Lo

Department of Forest Sciences

The University of British Columbia

Executive Summary

Mountain pine beetle (MPB) outbreaks can produce significant economic and ecological impacts over extensive areas. A current outbreak has affected stands through much of southern and central British Columbia, and there are concerns that the outbreak may spread east of the Rocky Mountains and into the extensive boreal Jack pine forest. There is a pressing need for a better understanding of the factors controlling these outbreaks and the potential effects of future climatic conditions.

Outbreaks may occur when two conditions exist: (1) favourable climatic conditions, and (2) pine stands that have achieved a vulnerable stage of development (typically aged between 80 and 160 years). The primary objective of this project was to examine climate-related influences at an annual time scale; previous studies have used climate normals to define climatic suitability. A second objective was to examine whether changes in climatic favourability for MPB spread can be related to larger-scale climatic phenomena, such as the Pacific Decadal Oscillation and El Niño-Southern Oscillation. A third objective was to examine stand-scale responses to climate that may influence their susceptibility to MPB infestation.

An approach to the prediction of the spatial and temporal variations in climatic favourability for MPB was developed by combining a model for interpolating daily precipitation and air temperature data in areas of complex terrain with favourability indices adapted from those used by Safranyik et al. (1975) and Carroll et al. (2004), which were based on climate normals. A key difference between the normal-based indices and those employed in this study was the use of a seasonally varying threshold for cold mortality. When applied to the Chilcotin outbreak in the 1970s and 1980s, the approach revealed statistically significant skill in identifying cell-years that were climatically favourable and thus had a higher probability of increased infestation. However, increased infestation was frequently observed in cells that were predicted to be climatically unfavourable. Causes for prediction error include (1) errors in the interpolated weather observations, (2) occurrence of favourable microclimatic settings (e.g., warm, south-facing aspects, areas of deep snow that would insulate the lower portions of tree trunks from severe cold) even in areas with unfavourable macroclimatic conditions, (3) uncertainty in the threshold values used in the indices and (4) effects of MPB population dynamics (e.g., density-dependent processes).

The approach was also applied to three transects crossing the Rocky Mountains in the vicinities of Banff, Jasper and Pine Pass. Observed outbreak patterns for all three transects were broadly consistent with the computed favourability indices. Winter cold mortality appeared to be the most frequent limiting factor for

MPB expansion. However, annual heat accumulation was also frequently below the threshold for favourability at the highest points on the Banff transect (Kicking Horse Pass, Lake Louise, Bow Valley). The years 1999 to 2001 were dominantly favourable at all sites, and this sequence of favourable years likely provided the conditions required for establishment of MPB on the east side of the Rockies.

The time series of the climatic favourability indices suggest that winter cold mortality played a dominant role in controlling MPB spread through the period since 1948. For example, the Chilcotin outbreak appears to have ended abruptly as a result of early cold snaps in the autumns of both 1984 and 1985. To examine the climatology of cold mortality events, synoptic circulation patterns based on daily grids of mean-sea-level pressure (MSLP) were classified into 13 types using a standard pattern-recognition technique. It was found that the circulation type representing Arctic outbreak conditions had the most frequent association with potential cold-mortality events throughout the province, though other types played a role in northern British Columbia.

There did not appear to be simple trends in synoptic-type frequencies. However, the interannual variations in the frequencies were significantly associated with different phases of large-scale ocean-atmosphere teleconnections, including El Niño-Southern Oscillation (ENSO), Pacific North America pattern (PNA) and the Pacific Decadal Oscillation (PDO). In particular, the frequencies of the synoptic types associated with potential cold-mortality events were lower in the neutral and positive phases of PDO, which have dominated since the occurrence of a major regime shift in 1976-1977. Furthermore, the conditional probability of having a day with temperatures below the cold-mortality threshold, given the occurrence of a "cold" synoptic type, was lower in neutral and positive phases of PDO. Therefore, the net effect was that the dominance of neutral and positive phases of PDO since 1977 has been associated with less frequent and less severe cold spells and hence greater favourability for MPB expansion. The climate changes associated with the PDO shift therefore appear to provide a reasonable proximal explanation for the more favourable winter climate. However, it is possible that the PDO shift is, itself, only one manifestation of a larger-scale climate phenomenon.

The lack of readily available climate-change scenarios that provided daily output prohibited the application of the favourability indices developed in this study for the examination of the potential for future MPB spread. However, the association between decreased winter cold mortality and the dominance of neutral and positive phases of PDO suggests that, unless there is a shift back to dominance by the negative phase of PDO (which was the case prior to about 1922 and between about 1947 and 1976), winter climatic conditions are unlikely to limit the spread of MPB throughout central British Columbia.

Progress has been made in relation to development of the FORECAST stand-level model to accommodate climatic change scenarios and allow prediction of stand-level controls on MPB dynamics. Work on that component of the study is still in progress and should be complete by the end of 2005. However, given recent findings concerning MPB attack in juvenile stands, it appears that populations may have reached a level for which stand-level characteristics are no longer a critical controlling factor, at least for the currently infested areas.

Further research is needed to improve the predictive accuracy of climatic favourability indices, including work on MPB biology and population dynamics to define more precisely the climatic thresholds for expansion. Further research is also needed on the calculation of the climatic favourability indices. Improved methods are required for interpolation of minimum daily air temperature from existing weather data, particularly to account for effects of cold air drainage and ponding during the extreme conditions that can cause mortality. These methods should account for the prevailing synoptic conditions and the topographic settings of the weather stations. In addition, approaches are required for predicting the effects of microclimatic variability on temperatures within the bark. Further studies should address the role of density-dependent processes and their influences on MPB spread, and how these interact with climatic conditions and stand-level attributes.

Table of Contents

Acknowledgments

1 Introduction

Mountain pine beetle (MPB) outbreaks can produce significant economic and ecological impacts over extensive areas. A current outbreak has affected stands through much of southern and central British Columbia, and there are concerns that the outbreak may spread east of the Rocky Mountains and into the extensive boreal Jack pine forest. There is a pressing need for a better understanding of the factors controlling these outbreaks and the potential effects of future climatic conditions.

Outbreaks may occur when two conditions exist: (1) favourable climatic conditions, and (2) pine stands that have achieved a vulnerable stage of development (typically aged between 80 and 160 years). Researchers at Canadian Forest Service (Allan Carroll, Stephen Taylor and Jacques Régnière) have made significant progress toward understanding the development of recent outbreaks in western Canada and the outlook for future outbreaks in the context of projected climatic changes. That work has been presented at conferences, but has not yet been published in peer-reviewed outlets. The researchers used the model BioSIM to map the distribution of climatically favourable sites on the basis of 30-year climate normals. They found that areas of favourable climatic conditions have expanded within western Canada since 1970, accompanied by increasing numbers of outbreaks within areas that had previously been climatically unfavourable. They have also shown that fire suppression through the twentieth century has created a large and spatially extensive cohort of lodgepole pine trees within the vulnerable age classes.

The primary objective of this project was to examine climate-related influences at a finer time scale (annual) than has previously been attempted, to provide a basis for incorporating climate information into models of MPB spread currently being developed by Brian Aukema, Allan Carroll, Jun Zhu, and Yanbing Zheng from CFS and the University of Wisconsin. A second objective was to examine whether changes in climatic favourability for MPB spread can be related to larger-scale climatic phenomena, such as the Pacific Decadal Oscillation and El Niño-Southern Oscillation. A third objective was to examine stand-scale responses to climate that may influence their susceptability to MPB infestation. Associated with these objectives are three goals:

(1)   To test indices of interannual variations in climatic favourability for mountain pine beetle. Achievement of this goal involved the following activities:

- Assemble climatic and spatial data bases
- Develop and test an interpolation model for daily climate data

- Develop and test climatic favourability indices for MPB

(2)   To relate recent changes in climatic favourability and mountain pine beetle outbreaks to synoptic- and larger-scale climatic phenomena, including El Nino-Southern Oscillation (ENSO), Pacific Decadal Oscillation (PDO) and Pacific North America (PNA) circulation pattern. Achievement of this goal involved the following activities:

- Conduct synoptic classification of daily weather patterns
- Correlate MPB climatic drivers with synoptic-scale weather types and large-scale teleconnection indices

(3)   To adapt and calibrate an existing stand-level forest ecosystem model (FORECAST) to simulate the effects of projected future climate change on stand development and mountain pine beetle habitat supply within individual forest stands. The modified model will be linked to the CFS bark beetle risk models and MoF risk rating system to simulate the combined and interacting effects of natural disturbance, climate change and stand management on the risk of MPB as a function of tree size, age and stress condition and temperature/precipitation regimes. The stand level FORECAST will be linked to a CFS fire model and to a large landscape model (using ATLAS and/or SELES) to examine the interacting effects of climate change, MPB, fire and harvesting.

2 Climatic variability in BC: data sources, processing and preliminary analysis

This section provides an overview of the data sources used to characterise climatic variations in BC, with a focus on the period beginning in 1948. It describes the collation, processing and preliminary analysis of surface climate data such as air temperature, as well as synoptic-scale circulation patterns and large-scale indices of ocean-atmosphere conditions. This section also describes the climate interpolation model used to compute time series of climatic favourability indices at points of interest throughout the province.

2.1 Surface climate data

Station observations of daily maximum temperature (T_{max}), daily minimum temperature (T_{min}) and daily total precipitation (P) were obtained from three different sources: Environment Canada's climate network (EC), The Ministry of Forests Fire Weather Station Network (FW), and the Ministry of Water, Land and Air Protection's Snow Pillow sites (SP). Table 2.1 provides an overview of the characteristics of this database of surface climate variables.

Table 2.1. Sources of surface climate data

Source	Dataset	No. of stations	Time period	Comments
Environment Canada	Canadian Climate CD West	1601(BC) 21 (YT, NWT) 230 (AB)	Variable (longest since 1880)	
Ministry of Forests Protection Program	Fire Weather Station Network	283 (310)	Since 1990s	Summer data only (winter not maintained, no T below –20 °C)
Ministry of Water, Land and Air Protection	Archived Automatic Snow Pillow (ASP)	68	Since late 1980s or early 1990s	Precipitation data inaccurate, all at higher elevations (1700 m $\pm$ 1000 m)

Figure 2.1 shows some characteristics of the station distribution in space and time. Stations are distributed unevenly across BC, with lower density towards the north. Many series are short: only 47 Environment Canada stations have a continuous record of temperature and precipitation data (with less than 5 years missing) covering the desired study period from 1950-2003. The Fire Weather network and the Snow

3

Pillow stations were established relatively recently. At the same time, the EC network was reduced. This reduction, together with the gaps and seasonally limited observations of the two smaller datasets, result in an effective decrease of climate observations in recent years, despite the increasing number of stations. A further problem is that most stations are located at low elevations. The few high-elevation stations are mainly the snow pillow stations, which do not have very long series and no reliable rainfall observations.
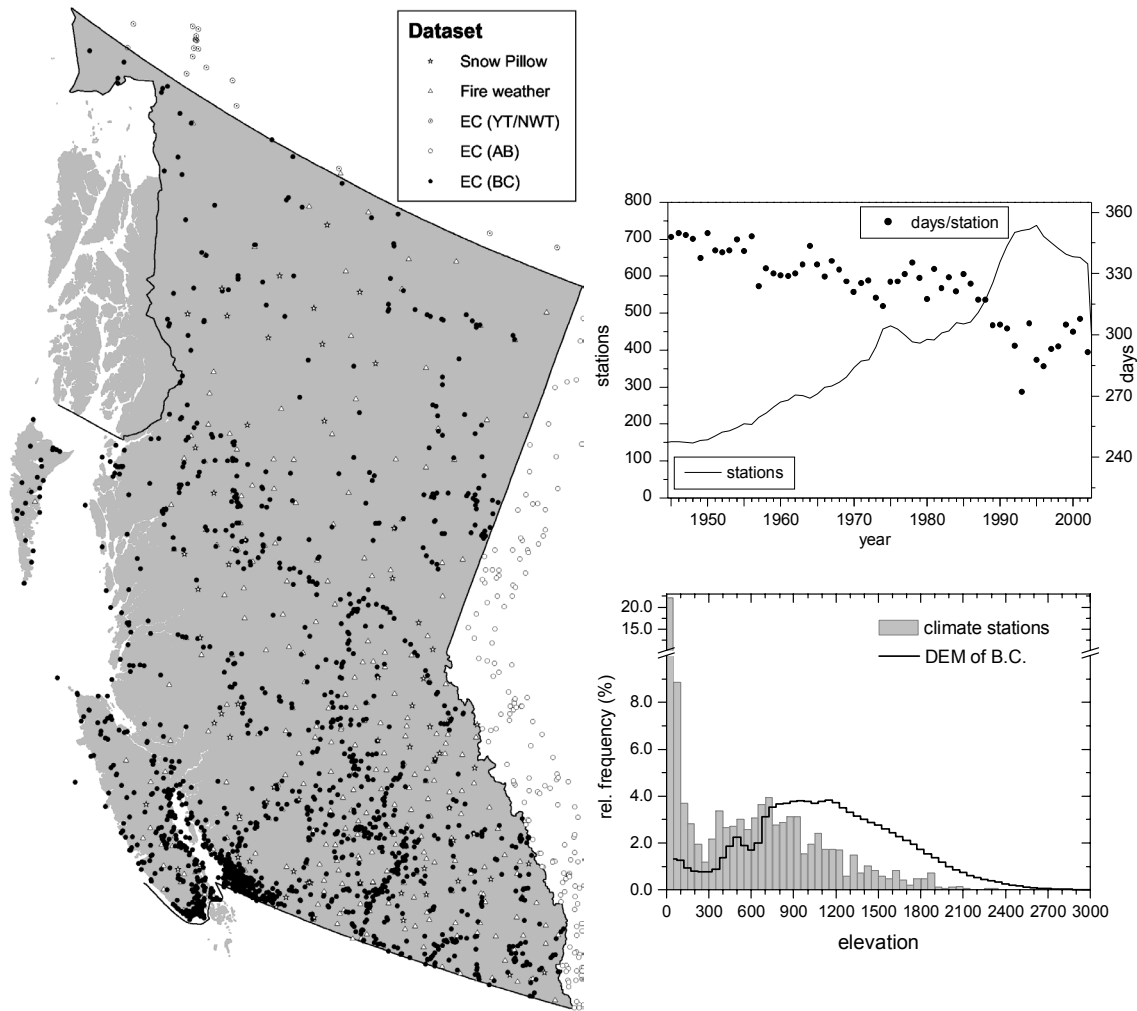

Figure 2.1. Distribution of stations: space, time and elevation

4

2.2   Climate Interpolation Model

Computation of the climatic favourability index for a location of interest requires the interpolation/extrapolation of climate data from the irregularly spaced station network. A variety of techniques have been developed for interpolating and extrapolating climate data, including simple extrapolation from a single base station, spatial regression, inverse-distance weighting and geostatistical methods such as kriging (e.g., Running et al., 1987; Holdaway, 1996; Thornton et al., 1997; Nalder and Wein, 1998; Bolstad et al., 1998). The method used in this project largely follows that of the DAYMET model developed by Thornton et al. (1997), which has been tested for daily climate data in the western United States (Thornton et al., 1997) and Austria (Hasenauer et al., 2003), both areas of complex, mountainous topography.

2.2.1   Methods

A Climate Interpolation Model (CIM) that uses the surface climate database collated for BC was programmed in Visual Basic. Three methods are available to interpolate daily temperatures for any given point: (a) a nearest neighbour approach with a specified temperature gradient; (b) the DAYMET temperature interpolation method; and (c) the DAYMET method with temperature gradients constrained by specified values for prediction points whose elevations lie outside of the elevation range of the predictor stations.

In the nearest neighbour interpolation method, the predictor station closest to the prediction point is used to specify T_0, the nearest known temperature (°C). The temperature at the prediction point, T_p (°C), is estimated as:

$$T_p = T_0 + G(h_p - h_0) \qquad\qquad [2.1]$$

where G is a specified temperature gradient (°C m^{-1}), h_p is the elevation of the prediction point (m) and h_0 is the elevation of the predictor station (m). An equation analogous to [2.1] could be used to estimate daily precipitation, but is not currently incorporated into the model.

The DAYMET method uses an iterative station density algorithm to determine a local set of predictor stations for each given prediction point, each with a weight that decreases with distance from the prediction point. Temperature and precipitation gradients are calculated by summing the weighted contribution of the temperature or precipitation gradient computed from every possible pair of predictor stations. The interpolation weights are computed for all stations in the database using a truncated Gaussian filter. From Thornton et al. (1997), the weights are given by:

$$W(r) = \begin{cases} 0; & r > R_p \\ \exp\left[-\left(\dfrac{r}{R_p}\right)^2 \alpha\right] - e^{-\alpha}; & r \le R_p \end{cases} \qquad [2.2]$$

where $W(r)$ is the weight associated with the radial distance r from the prediction point p, R_p is the truncation distance from p, and α is a unitless shape parameter. The truncation distance R_p is allowed to vary so that it may be reduced in areas of high station density and increased in areas of low station density. The user specifies a desired number of observations N, and the model uses an iterative scheme to vary R_p such that the actual number of observations used in the interpolation converges towards this value of N. The reader is referred to Thornton et al. (1997) for details of the iterative estimation of the local station density and subsequent adjustment of R_p. Following the truncation distance adjustment, interpolation weights are calculated and then used in the temperature and precipitation interpolations, as described below.

Because many of the recording stations operated either intermittently or only for short periods, the set of stations reporting data varied through time. To maximize the use of this patchy network, the interpolation model calculates station weights for each day in the database separately. This procedure differs from previous implementations of the DAYMET model where station densities are calculated on an annual basis using an annually fixed network of stations (e.g. Hasenauer et al., 2003). The daily calculations allow data from a changing network of weather stations to be used with no assumptions made as to the temporal continuity of the data station network. However, this approach greatly increases computing time.

In the DAYMET model, T_p is interpolated using information from all stations with non-zero interpolation weights. A weighted least-squares regression is used to determine the local temperature

gradient. Each unique pair of stations is assigned a regression weight equal to the product of the interpolation weights of the two stations in the pair. The regression model takes the form

$$(T_1 - T_2) = \beta_0 + \beta_1(h_1 - h_2) + \varepsilon \qquad [2.3]$$

where subscripts 1 and 2 refer to the two stations in the unique pair, and β_0 and β_1 are the regression coefficients, and ε is the error term. Once the regression coefficients are calculated, T_p is predicted by:

$$T_p = \frac{\sum_{i=1}^{n} W_i \left[T_i + b_0 + b_1(h_p - h_i) \right]}{\sum_{i=1}^{n} W_i} \qquad [2.4]$$

where b_0 and b_1 are the estimated regression coefficients, h_p is the elevation of the prediction point and the subscript "i" refers to the predictor stations.

In regions of mountainous terrain, there will be locations that are either above or below the elevation range of the local weather station network. In such locations, the DAYMET temperature calculation becomes an extrapolation with respect to h. In order to prevent extrapolations from predicting unrealistic temperatures at high elevations, a third method, the constrained DAYMET option, computes the temperature gradient using a weighted average of the gradient computed by DAYMET (b_{1D}) and a specified gradient (b_{1S}). The specified temperature gradient can be set manually or a text file can be loaded that contains monthly lapse rates. This option computes the gradient as

$$b_1 = W_D b_{1D} + W_S b_{1S} \qquad [2.5]$$

where the weights are computed as

$$W_D = \begin{cases} (z_{max} - z_{min})/(z_p - z_{min}), & z_p > z_{max} \\ (z_{max} - z_{min})/(z_{max} - z_p), & z_p < z_{min} \end{cases} \qquad [2.6]$$

and

$$W_s = 1 - W_D \qquad\qquad\qquad [2.7]$$

where z_{max} and z_{min} are the maximum and minimum elevations of the predictor stations and z_p is the elevation of the prediction point.

Specified lapse rates were estimated on a monthly basis by identifying six pairs of low-elevation/high-elevation stations that were reasonably close (within a few tens of km) and computing vertical temperature gradients from them. An average was computed for each month, which was used in the constrained DAYMET algorithm.

For precipitation interpolation only the DAYMET method is available. That algorithm uses a two-step procedure. In the first step, the probability of precipitation for the prediction point is estimated based on the occurrence of precipitation at neighbouring stations. A daily precipitation value of 0 is assigned if the probability falls below a threshold value. If the probability lies above the threshold, then a precipitation total is interpolated from surrounding stations. Interpolation calculations use the same weighted-regression approach as for temperature. See Thornton et al. (1997) for further details.

2.2.2   Testing

The model was cross-validated for two selected years with differing data availability: 1965 and 2000. For each day, each station was, in turn, withheld from the set of control points and was predicted by interpolating from the other stations. The prediction error was aggregated over all stations and was expressed as both Mean Absolute Error (MAE) and Root Mean Squared (RMS) error. Table 2.2 summarizes the MAE for the three interpolation models and for BC stations only (some stations in Alberta and the Yukon and Northwest Territories were also used for the interpolation to reduce edge effects).

Table 2.2 Mean absolute error (°C) of temperature predictions for BC stations for different model validations

Model	2000		1965	
	T_{max}	T_{min}	T_{max}	T_{min}
Nearest neighbour	1.55	1.94	1.57	1.97
DAYMET	1.45	1.75	1.57	1.93
Constrained DAYMET	1.42	1.73	1.54	1.89

8

All models performed better for 2000 than for 1965 and predicted T_{max} more accurately than T_{min}. The nearest neighbour model showed the poorest performance, DAYMET took the middle place and its constrained version performed best. However, the differences in MAE between the models are all less than 0.2 °C. The RMS errors (not shown) indicated the same ranking. Although the mean absolute errors were small, individual days can have large errors (Figure 2.2). In Figure 2.2, the sharp drop in the number of data points below -20 °C for T_{min} reflects the characteristics of the fire weather station network dataset. Most fire weather stations do not record data at all during the winter months, and some cannot measure temperatures below -20°C. In the latter case, all days colder than this threshold were recorded as missing values.
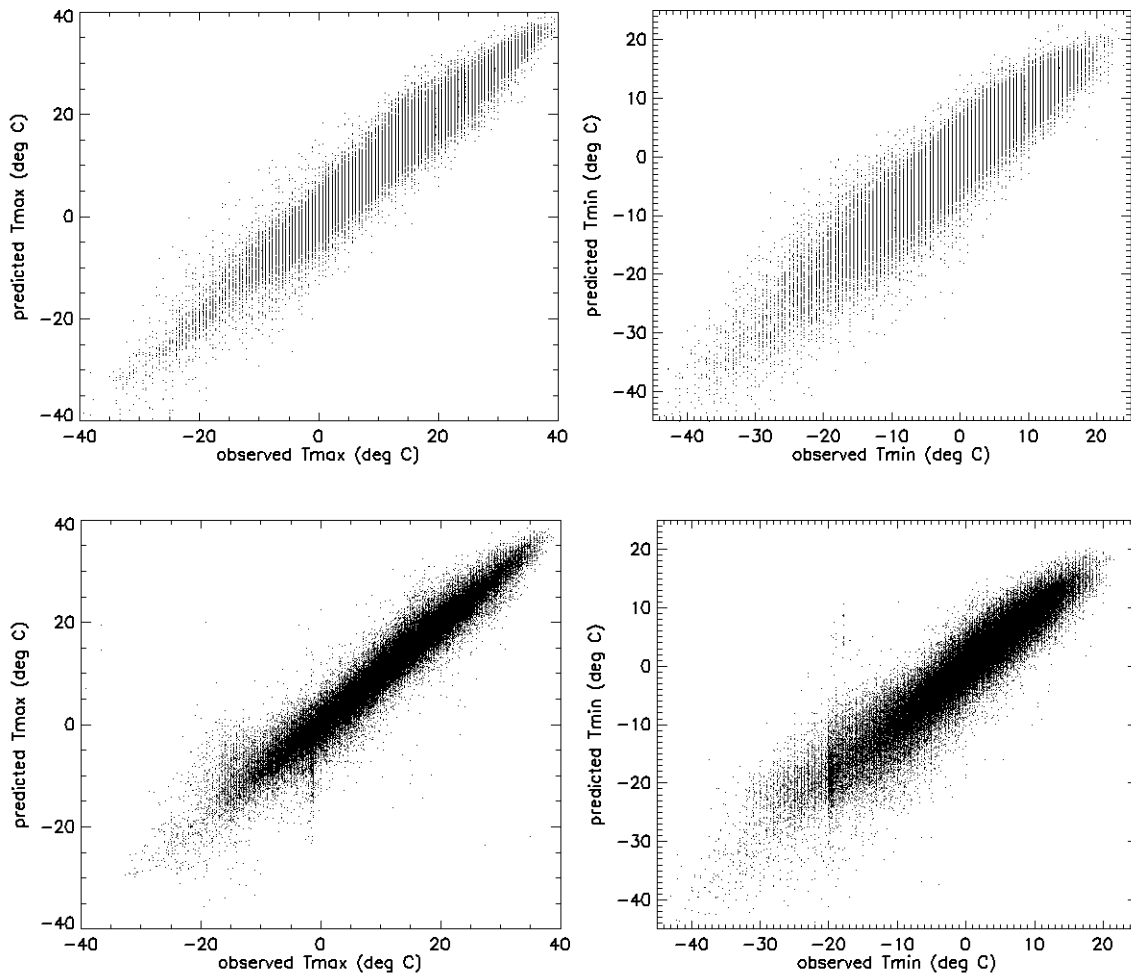

Figure 2.2 Observed vs predicted T_{min} and T_{max} values for the year 1965 (upper panels) and 2000 (lower panels).

9

It is important to assess the performance of the model for different elevation ranges, given that the network has a low density of high-elevation stations relative to the distribution of land area in BC (Figure 2.1). As can be seen in Table 2.3, low-elevation stations had lower MAE, as expected from the higher station density. In 2000, with the Snow Pillow and Fire Weather stations available, the dataset contained more high elevation stations than in 1965, and the differences in model performance reflect the differences in station distribution. For 1965, the basic model for T_{min} performed slightly better than the constrained model and much better than the DAYMET model, which appeared to calculate inaccurate temperature gradients in the absence of high-elevation control points.

Figures 2.3 and 2.4 show the spatial distribution of MAE of the best overall model (constrained DAYMET). In 1965, in particular, the impact of the varying station density is visible. MAE values were much higher in the northern part of the province where station density was low. Large errors in T_{max} occurred on the north coast, while T_{min} appeared more difficult to predict than T_{max} on the central plateau areas.

Table 2.3 Mean absolute error (°C) of temperature predictions stratified by elevation range

| Model and year		Elevation range			
		< 500 m	500 m to 1000 m	1000 m to 1500 m	>1500 m
1965					
Nearest neighbour	T_{max}	1.49	1.62	1.88	2.60
	T_{min}	1.71	2.31	2.53	3.51
DAYMET	T_{max}	1.44	1.62	2.15	3.47
	T_{min}	1.59	2.26	2.88	5.62
Constrained DAYMET	T_{max}	1.44	1.60	2.03	2.49
	T_{min}	1.59	2.21	2.78	3.57
2000					
Nearest neighbour	T_{max}	1.34	1.45	1.87	2.39
	T_{min}	1.50	2.02	2.46	2.78
DAYMET	T_{max}	1.28	1.40	1.67	2.04
	T_{min}	1.43	1.89	2.11	2.05
Constrained DAYMET	T_{max}	1.26	1.40	1.59	1.99
	T_{min}	1.42	1.89	2.05	2.00
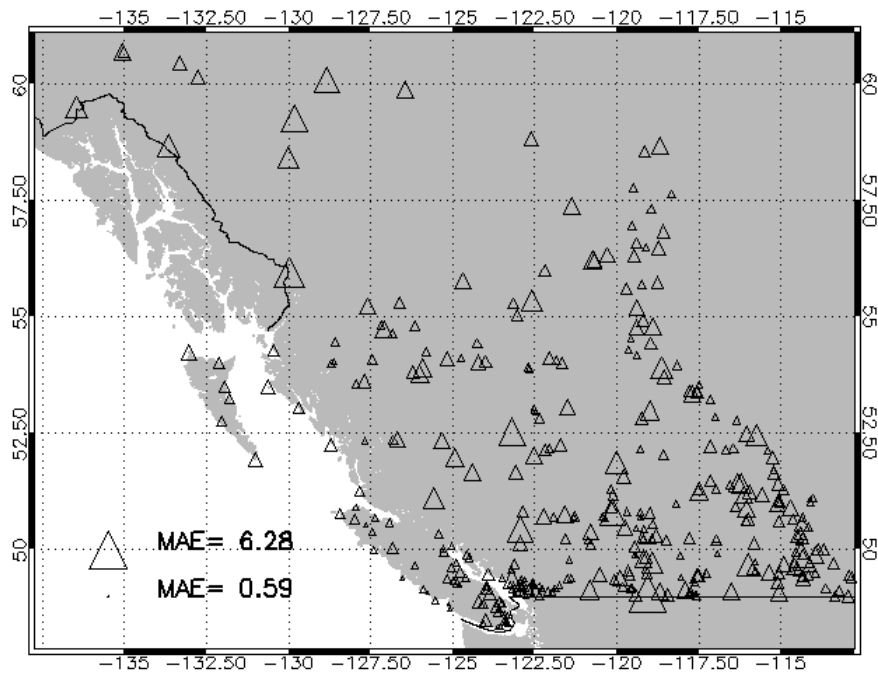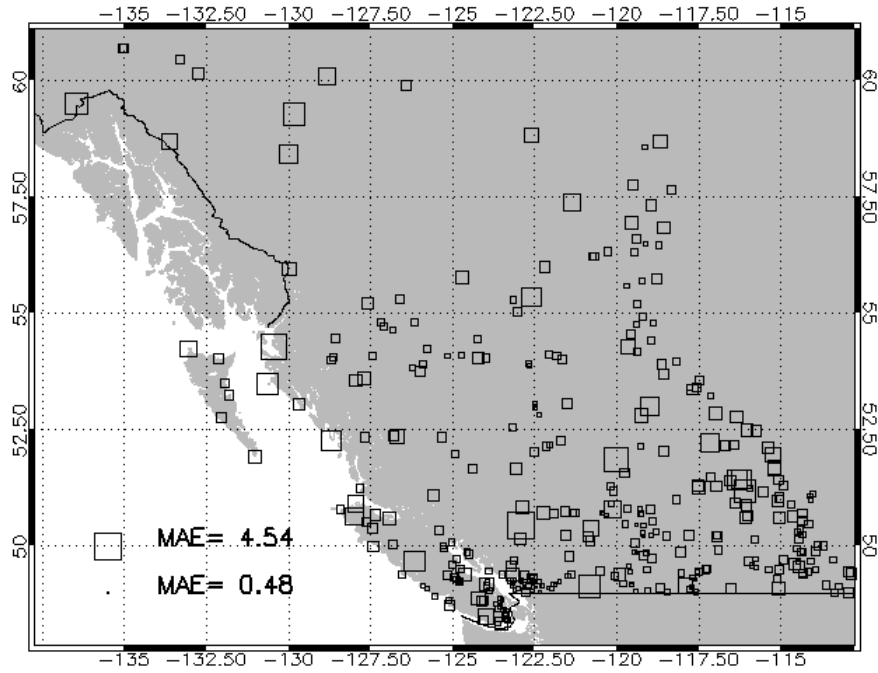
Figure 2.3 MAE at each station for the validation of T_{max} (upper panel) and T_{min} (lower panel) in 1965
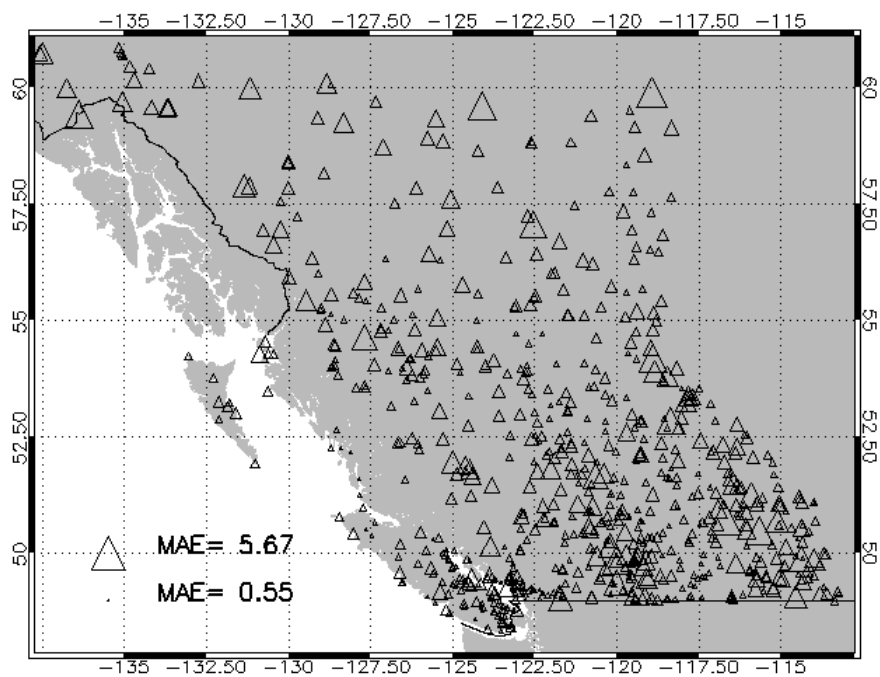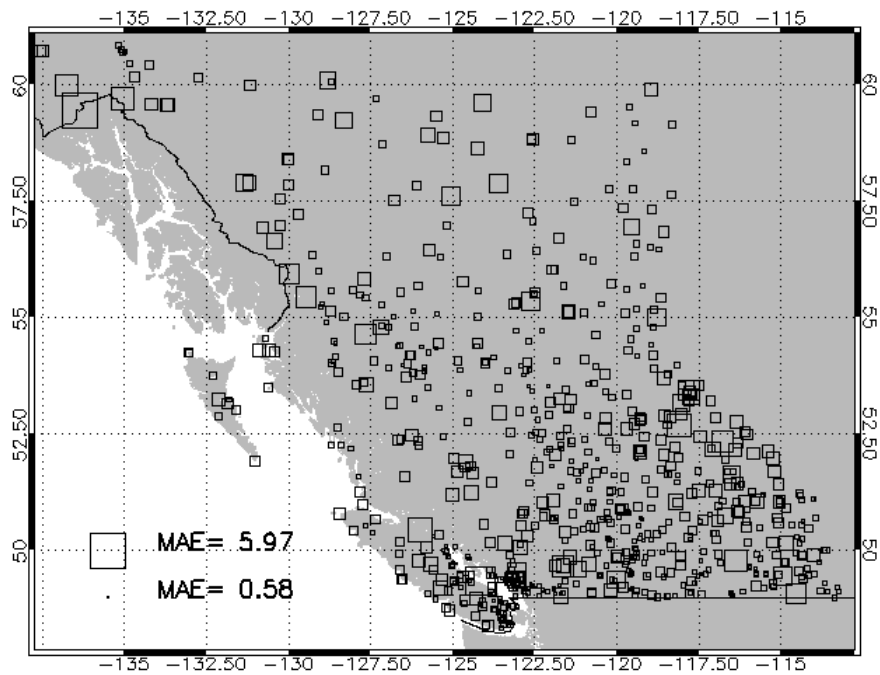
Figure 2.4 MAE at each station for the validation of T_{max} (upper panel) and T_{min} (lower panel) in 2000

2.2.3   Discussion of model performance

The constrained model generally performed best for both validation years and is therefore the preferred interpolation method. The MAE values for the cross-validation of the constrained model for the year 2000 varied from 1.4 to 2 °C for all elevation ranges. For the year 1965 the model was somewhat less accurate. Considering the size of BC and the complexity of the terrain, however, these values of MAE are reasonable, and are similar to those attained by Thornton et al. (1997) and slightly greater than those obtained by Hasenauer et al. (2002) in areas with higher densities of high-elevation stations.

The poorer performance for minimum temperature is likely related to the influences of cold air drainage and ponding during cold periods. These phenomena can invert vertical temperature profiles and thus complicate the extrapolation of air temperature to higher elevations from low-elevation stations. Further research should focus on methods for temperature interpolation and extrapolation that can account for differences in topographic influence under different seasons and synoptic situations.

2.3   Synoptic classification

2.3.1   Data and method

To improve the understanding of the causes of recent climatic variability and possible related changes in climatic favourability for MPB, a circulation-to-environment synoptic climatology approach (Yarnal, 1993) was employed, in which a set of synoptic circulation patterns is derived solely based on atmospheric data. These patterns were then related to surface climate across BC.

Mean-sea-level pressure (MSLP) and geopotential height (GPH) data for this purpose were extracted from archives maintained by the NOAA-CIRES Climate Diagnostics Center (CDC), Boulder, Colorado, USA, from their web site at http://www.cdc.noaa.gov/ . These data originate from the global National Center for Environmental Prediction (NCEP) Reanalysis Project. The NCEP data used in this study are daily averages on a 0.5° (latitude and longitude) grid since 1948. From these, a 20 x 10 grid was extracted that covers the North Pacific and British Columbia between 157.5°W and 110.0°W and 40°N and 60°N.

Daily circulation patterns were classified using *Synoptic Typer 2.0*, an application by the Australian Bureau of Meteorology (Dahni, 2004). Daily grids of MSLP from 1948-2003 were subjected to a commonly used pattern recognition scheme using principal component analysis (PCA) followed by an

unsupervised k-means cluster analysis on the components scores of the retained components (Dahni and Ebert, 1998). The output includes a catalogue of daily circulation types for each day of the study period. From this catalogue, circulation type frequencies can be derived for specific seasons and/or sub-periods, thereby permitting analysis of the overall frequencies of the daily types, their seasonal variability, and their duration and transition probabilities.

2.3.2   Synoptic types and surface climate

The classification procedure produced 13 distinct circulation types. These are best illustrated by composites, which are the mean MSLP patterns for each type (Figure 2.5). Types 1 and 2 were the most frequent circulation types. They occur year-round, but dominate BC's synoptic climatology during the summer months. From June to September, these two circulation patterns, together with Type 8, made up more than 50% of the days. The MSLP patterns of these three types show the high pressure influence in BC with the Hawaiian High just off the coast. The mainly meridional flow over BC (Types 1 and 2) is typical for dry and fine summer weather, whereas the southern position of the High in Type 8 causes more zonal flow with unstable weather.

During autumn, winter and spring, BC's synoptic climatology is more variable, and most of the circulation types occur with a similar frequency between November and February. Circulation types 3 to 7 are distributed most evenly throughout the year, but all have a minimum in summer. They represent a mix of patterns and influences on BC climate. The Aleutian Low is visible in most of the patterns; however, it is either not strong (Type 3) or located on the westmost edge of the domain. This pattern leaves BC (particularly the interior and the north) under the influence of continental high pressure ridges from north or south. Perhaps with the exception of type 6, however, which has a high persistence, these patterns are not very stable and tend to be transitional situations within the typical mid-latitude circulation characterized by series of frontal systems moving from west to east. Types 9 through 13 occur mainly in winter. They are all characterized by an eastward-shifted Aleutian Low of varying location and depth. Southwesterly flow over BC is common during these situations.
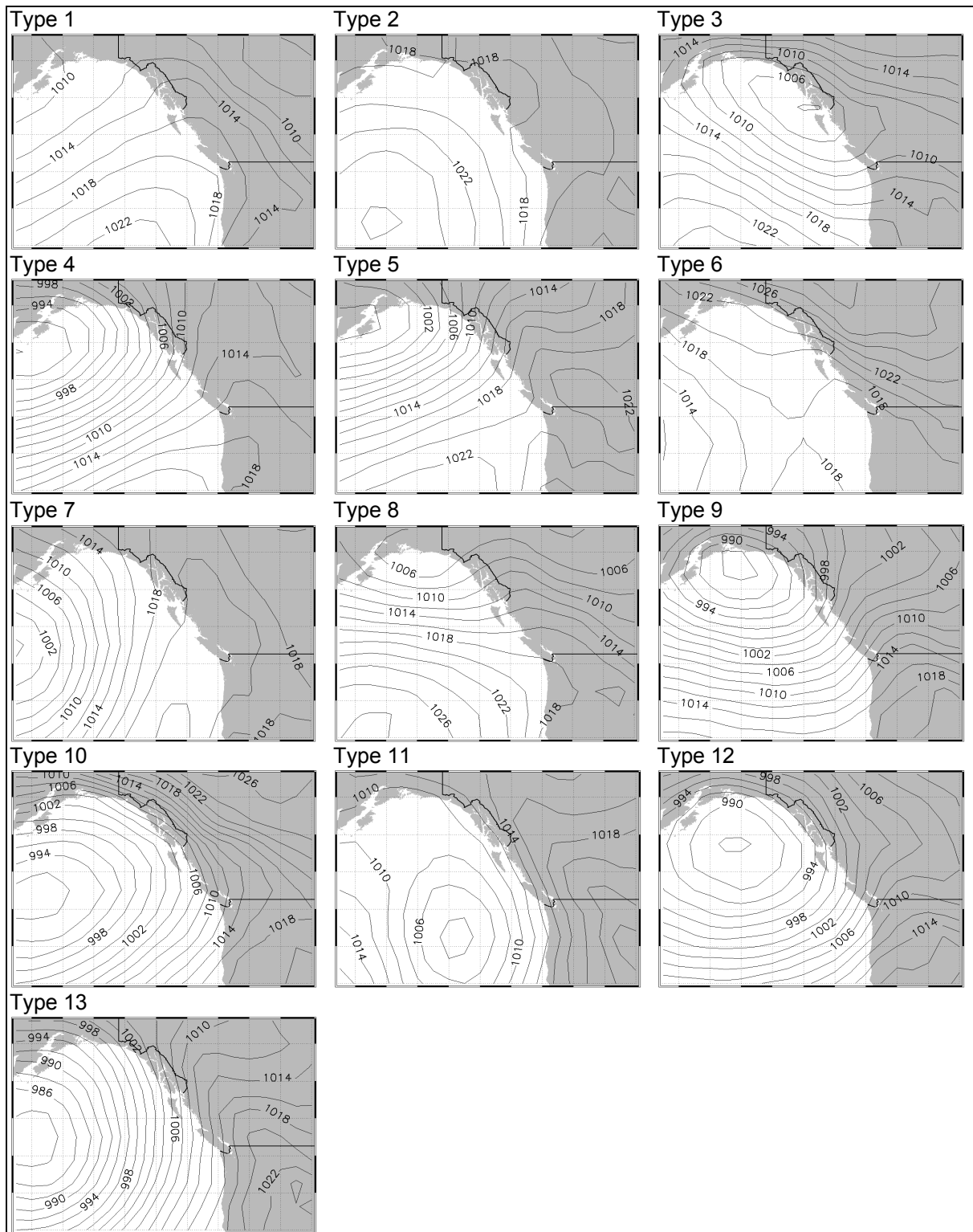
Figure 2.5. Composites of the mean-sea-level pressure patterns for the 13 circulation types. Surface pressures are in hPa.

To characterize the surface climate patterns associated with the different synoptic types, minimum and maximum temperature and precipitation statistics at 43 weather stations with long records were analyzed. Daily temperatures were first standardized by their monthly mean and standard deviation, and then average z-scores calculated at each station for each circulation type for four seasons (DJF, MAM, JJA, SON), as well as the winter (Oct-March) and summer (April-Sep) half-years. To express precipitation anomalies, seasonal amounts for each circulation type were calculated as a percentage of the long-term seasonal mean. Figure 2.6 shows some examples. Winter temperatures for type 6, which describes an Arctic outbreak situation, are much lower than normal, especially for central to northern BC. For type 10 the Arctic influence is only evident in northern BC, while the southwest experiences higher than normal temperatures. Positive winter precipitation anomalies in eastern BC are associated with type 3.
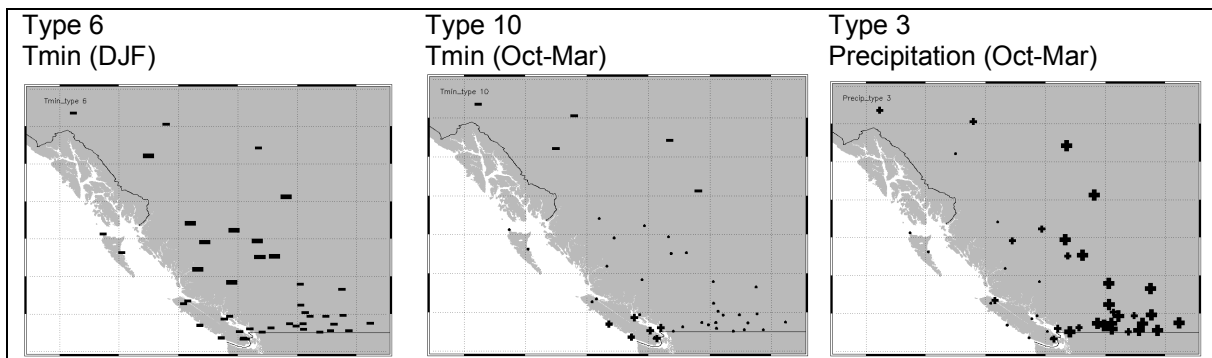

Figure 2.6. Selected seasonal surface climate anomalies. Positive and negative anomalies are indicated by "+" and "-" symbols, respectively. The size of the symbols is scaled to the absolute value of the anomaly.

2.3.3   Temporal variation in synoptic type frequencies

The seasonal frequencies of the synoptic types varied considerably from year to year, particularly those of types 3, 8, 12 and 13 in winter. To test for trends, Kendall's tau rank correlation coefficient and the two-tailed significance of its deviation from zero were calculated for the annual series of seasonal frequencies from 1948 to 2003.

The winter frequencies of types 2, 3 (Figure 2.7) and 5 exhibit negative trends (tau between -0.11 and -0.16). The types are all associated with negative temperature anomalies. However, none of these negative trends is statistically significant at the 95% confidence level. Frequencies of types 7, 10, 12 and 13 show positive trends, with only those for types 7 and 13 being significant. These types are mainly associated

16

with positive temperature anomalies. Negative trends for the annual summer frequencies were found for types 3 and 5 and also for types 8 and 9. Trends for types 5 and 8 are significant at the 95% level. Positive trends were found for types 7, 10, and 13, and all are significant. The surface climates of these types do not show any common patterns.
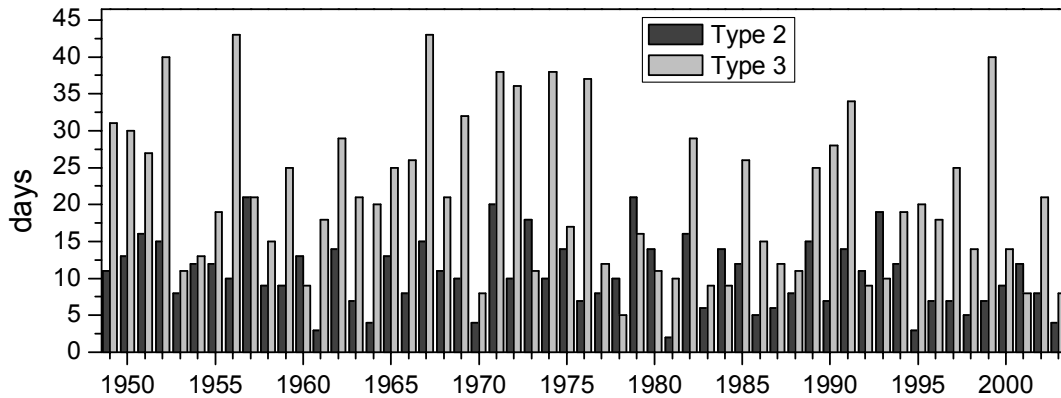

Figure 2.7. Winter frequencies of Type 2 and Type 3.

2.4 Large-scale climate indices

In order to explain the interannual to decadal variability of surface climate and synoptic types, it is useful to investigate links to larger-scale climate phenomena, which can be quantified by several teleconnection indices related to sea-surface temperatures or atmospheric circulation patterns. Time series of such indices are readily available, and they have been found to explain a significant proportion of interannual climatic variability in BC and adjacent areas of the United States (e.g., Redmond and Koch, 1991; Moore and McKendry, 1996; Shabbar et al., 1997; Shabbar and Bonsal, 2004). Large-scale indices have also been found to correlate with a broad range of environmental variables including snowpack accumulation, salmon dynamics and glacier mass balance (e.g., Moore and McKendry, 1996; Mantua et al., 1997; Bitz and Batisti, 1999; Moore and Demuth, 2001).

The Southern Oscillation Index (SOI), which describes the El Niño Southern Oscillation (ENSO) state by the standardized difference of MSLP between Tahiti and Darwin, is available from the CDC website. The Pacific Decadal Oscillation (PDO) index, which is the time series of scores for the leading principal component of the North Pacific SST variability (Mantua et al., 1997), can be downloaded from

17

http://tao.atmos.washington.edu/pdo/, the website of the University of Washington's Joint Institute for the Study of the Atmosphere and Ocean (JISAO). The positive (warm) phase involves warmer-than-average water along the western North American coast and cooler-than-average water in the central North Pacific. The negative (cold) phase has opposite anomalies.

Also available from JISAO are the Pacific North America Pattern (PNA) index, which describes the mid-tropospheric circulation over the North Pacific and North America (Wallace and Gutzler, 1981), and the Arctic Oscillation (AO) index, which represents the dominant pattern of non-seasonal sea-level pressure (SLP) variations north of 20°N (Thompson and Wallace, 1998). The PNA pattern is a natural, internal mode of circulation variability over the North Pacific and North America. The strong or enhanced (positive) phase is characterized by southerly air flow along the west coast of North America with a ridge of high pressure over the Rocky Mountains. The weak (negative) phase is dominated by westerly, zonal flow. Moore and McKendry (1996) found that the strong phase tended to coincide with warmer winters and reduced snowpack accumulation throughout BC.

The AO is associated with fluctuations in the strength of the winter stratospheric polar jet. Its index is computed as the time series of scores for the leading-mode principal component of SLP poleward of 20°N. A positive AO index value generally indicates negative and positive SLP anomalies in the Arctic and midlatitudes, respectively, and relatively strong 55°N (surface) westerlies; a negative index value indicates the opposite pressure anomalies and weaker westerly flow (Thompson and Wallace, 1998; Wallace and Thompson, 2002).

2.5 Climatic variations in BC in relation to large-scale indices and synoptic type frequencies

North Pacific teleconnections are strongest during winter (e.g., Trenberth, 1990). Data analyses were therefore concentrated on the winter season from December to February (DJF). For this study, years were classified (year 2000 being Dec. 1999 to Feb. 2000) into commonly used phases: El Niño and La Niña winter were defined by the preceding May to November SOI according to Redmond (2005); positive/negative PDO phases were defined by the DJF mean of the PDO index >0.5/<-0.5; and similar thresholds were applied to DJF averages of PNA and AO to define positive and negative years. Figure 2.8 illustrates the phases of the different indices. There was a major regime shift beginning in 1977, which was associated with a shift to a dominance of positive or neutral PDO and PNA phases. Earlier regime shifts occurred in 1922 and 1947 (Mantua et al., 1997).
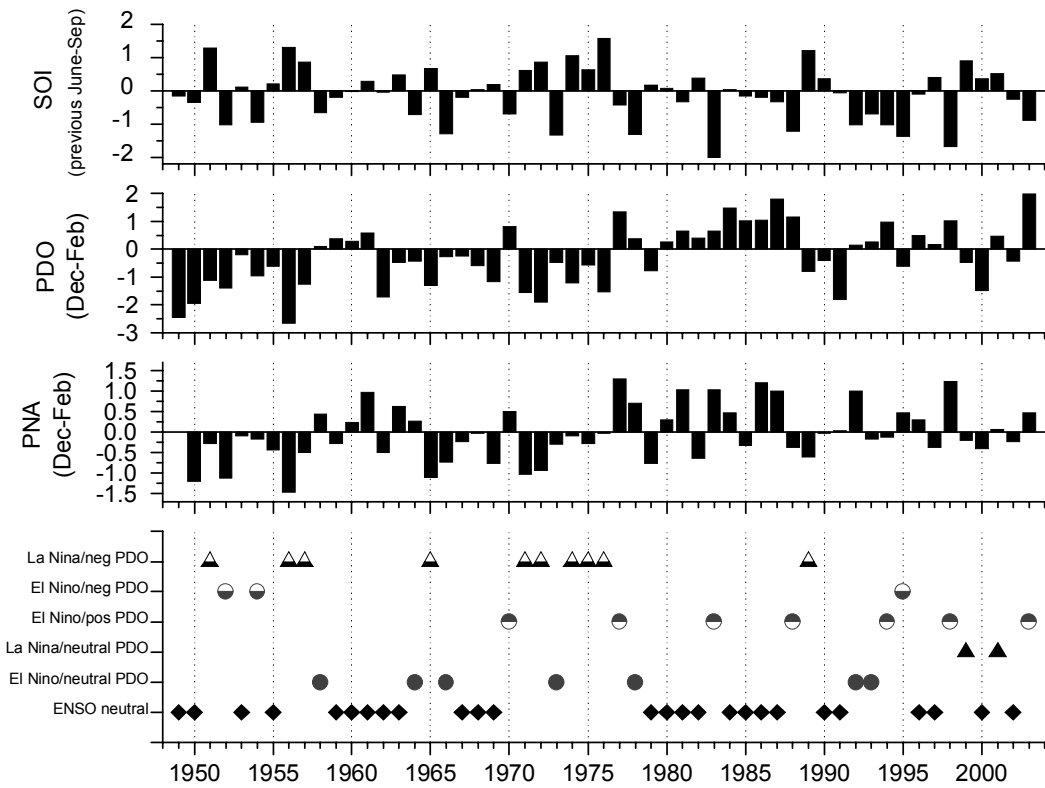
Figure 2.8. Time-series of large-scale index phases: DJF averages of PDO, AO and PNA, and classified combined ENSO/PDO phases

As shown in Table 2.4, mean winter temperature at selected stations varied significantly among the different phases of PDO, but significant differences associated with ENSO or the joint ENSO/PDO phases were only apparent for Prince George. A post-hoc test revealed that mean winter temperatures in neutral and positive PDO years were significantly higher than those in negative PDO years. Similar results were found for a comparison of annual mean minimum temperatures (Table 2.5). Analyses of variance (ANOVA) followed by a Tukey post hoc test revealed that the minimum winter temperatures showed significant differences at three out of seven stations for the ENSO phases (El Niño years being warmer and La Niña years being cooler), at all stations for the PDO phases (neutral and positive years being warmer than negative years), and at four out of seven stations for the combined ENSO/PDO classification (mainly El Niño/pos.PDO being warmer than La Niña/negative PDO).

19

Table 2.4. Results of ANOVA examining differences in mean winter temperature among different teleconnection phases. Values shown are significance levels associated with the null hypothesis of no difference.

Station number	Station name	ENSO	PDO	ENSO/PDO
1096450	Prince George	*0.041*	*< 0.001*	*0.024*
1125700	Okanagan	0.19	*0.002*	0.115
1183000	Fort St. John	0.186	*0.001*	0.102
1152850	Fernie	0.521	*0.016*	0.674

Table 2.5. Results of ANOVA for annual mean T_{min} values for different index phases*

Station	Location	ENSO		PDO		ENSO/PDO	
		p	sign. contrasts	p	sign. contrasts	p	sign. contrasts
1096450	Prince George	*0.026*	EN/LA	*<0.001*	n/neg, pos/neg	*0.015*	EN+pos/LA+neg
1108447	Vancouver	0.265		*<0.001*	n/neg, pos/neg	0.266	
1125700	Okanagan Centre	0.156		*0.001*	n/neg, pos/neg	*0.042*	EN+pos/LA+neg
1183000	Fort St. John	0.140		*<0.001*	n/neg, pos/neg	0.057	
1054500	Langara	*0.001*	EN/LA, n/LA	*<0.001*	n/neg, pos/neg	*0.002*	EN+n/LA+neg, nn/LA+neg, EN+pos/LA+neg
1032730	Estevan Point	*0.039*	EN/LA	*<0.001*	n/neg, pos/neg	*0.032*	EN+pos/LA+neg
1152850	Fernie	0.610		*0.005*	n/neg	0.897	

* EN= El Niño, LA= La Niña, nn=neutral ENSO, n=neutral PDO, pos=positive PDO, neg= negative PDO

There are two possible hypotheses to explain teleconnections between large-scale climate phases and surface climate in terms of synoptic climatology: (a) the frequencies of circulation patterns change with the index phases, or (b) the temperatures or precipitation amounts associated with different circulation patterns change. The first hypothesis was tested by applying a chi-square test of independence between the DJF frequencies of the synoptic types and the ENSO and PDO phases. The analysis showed clearly that the synoptic-type frequencies varied with the large scale index phases (Table 2.6, Figure 2.9). Types 2, 3, 10, 12 and 13 had a significant association with all indices. Types 6 to 8 were strongly associated with PDO and PNA and the combined ENSO/PDO index. The residuals indicated the direction of the association: e.g. types 10, 12 and 13 were more (less) frequent in positive (negative) PDO phases, while types 2, 3, 6 and 8 were less (more) frequent in positive (negative) PDO phases. The residuals for the

ENSO phases (not shown) were similar to those in Figure 2.8. The frequencies of types 10, 12 and 13 (which were associated with warm anomalies from predominantly southwesterly flow) and types 2, 3, and 6 (which were associated with cold anomalies and Arctic outflow situations) can therefore explain, at least to a certain degree, the finding that positive PDO phases and El Nino years were generally warmer and negative PDO phases and La Nina years were generally colder.

Table 2.6. Chi-square test for the association between synoptic type frequencies and large-scale climate index phases. Significant associations are indicated by x ($p < 0.05$) or xx ($p < 0.01$).

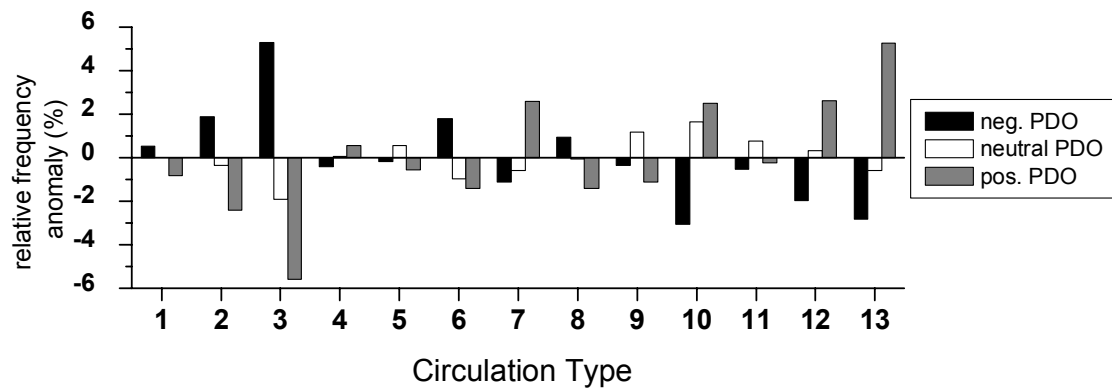| Type	ENSO	ENSO/PDO	PDO	PNA	AO
1				x	xx
2	xx	xx	xx	xx	xx
3	xx	xx	xx	xx	xx
4				x	
5					x
6	x	xx	xx	xx	
7		x	xx	xx	
8		xx	xx	x	
9			x	xx	xx
10	xx	xx	xx	xx	xx
11	xx	x			xx
12	xx	xx	xx	xx	x
13	xx	xx	xx	xx	xx

Figure 2.9. Residuals of the Chi-square test for association between winter synoptic type frequencies and PDO phase.

21

The second hypothesis was tested by comparing the daily minimum temperatures in different phases for individual circulation types. Because the data do not necessarily meet the ANOVA assumptions of independence, normality and homogeneity of variance, the analysis was limited to visual comparison of box plots. The analysis focused on types 2, 3, 5, 6, 10 and 11, which were frequent circulation patterns in winter and often associated with extreme cold. At all stations and for all six types, the minimum temperatures tended to be lower during negative PDO phases than during neutral or positive PDO winters (Figure 2.10 shows one example). However, the variability of the minimum temperatures during negative PDO phases at most stations was still high.

Based on the analyses reported above, the overall effect of ENSO and especially PDO on surface climate appears to result from the combination of changes in both the synoptic type frequencies and the within-type temperatures. However, there is still substantial variability in surface climate that is not simply associated with larger-scale conditions.
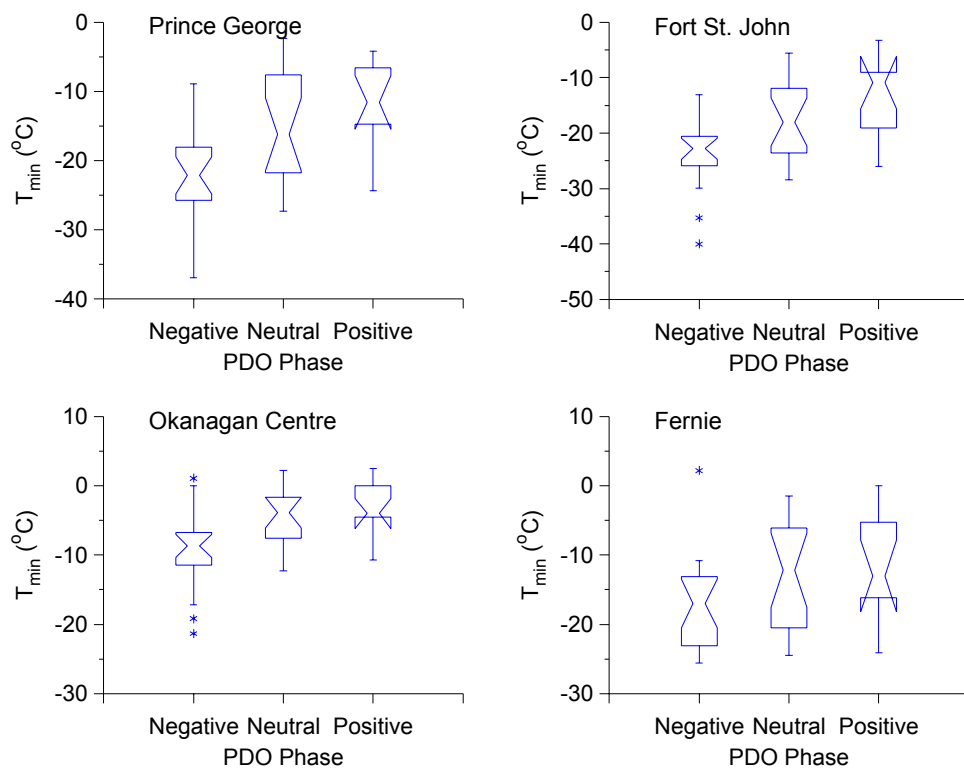

Figure 2.10. Distribution of daily DJF T_{min} values for Type 2 in different PDO phases.

3 Links between climate variations and Mountain Pine Beetle outbreaks

This section explores the linkages between climatic variability and the spatial and temporal variability of recorded MPB outbreaks. It outlines the spatial data used, the derivation of the climatic favourability indices, and the comparison of outbreak dynamics with variations in climatic favourability. Because current computing time constraints prohibit the calculation of gridded favourability indices for the entire province, the study focused on the Chilcotin outbreak of 1973-1985, then examined recent variations of climatic favourability for three passes over the Rocky Mountains (Pine Pass, Jasper and Kicking Horse), to evaluate their effectiveness as barriers to MPB range expansion. These passes are of particular interest because they are potential gateways through which MPB could spread or have recently spread across the Rockies and potentially into the extensive boreal jack pine forests (A. Carroll, Canadian Forest Service, pers. comm.).

3.1 Spatial databases used in analyses

Visual comparisons were based on the annual maps of MPB infestation from Taylor and Erickson (2003) as well as a coverage of the distribution of pine in BC in the year 2000 provided by Marvin Eng, BC Ministry of Forests Research Branch. A 77-m DEM for BC recently developed by Brian Klinkenberg, Department of Geography, UBC, from Shuttle Radar Topography Mission DTED data was used to assist with interpolation of daily surface climate data to a grid.

3.2 Calculation of climatic favourability indices

Safranyik et al. (1975) developed an index of climatic suitability based on relations between MPB life history, mortality and climatic variables, with temperature being the most important. A univoltine life cycle synchronized with critical seasonal events is essential for MPB survival (Logan and Powell, 2001). The index of climatic suitability was originally intended to determine the potential geographic range for MPB and was calculated from climate normals (Safranyik et al., 1975). Using a modified index and a stochastic weather generator to downscale daily weather conditions from climate normals, Carroll et al. (2004) examined changes in suitability for sequential 30-year periods, shifted over decades in their study. Their analysis showed that the recent expansion of the range of MPB is consistent with climatic changes.

They also applied the suitability model to projected future climate scenarios, and found that future climatic conditions may allow the recent range expansion to spread into the jack pine stands of the Canadian boreal forest.

An important goal of this project was to increase the resolution and examine the time series of the individual time-varying components of the climatic suitability index (the index also includes two time-invariant components) to identify the factor(s) that appeared to be most implicated in the observed outbreaks. This approach requires the use of observed daily data. The individual time-varying components of the index are summarized in Table 3.1. The calculation of the cold mortality criterion was slightly modified from Carroll et al. (2004) by using cold mortality curves established by Wygant (1937) as opposed to a fixed threshold of -40°C. These curves, shown in Figure 3.1, represent seasonally varying thresholds for initial, 50% and 100% mortality and were derived from laboratory experiments. Mortality occurs at much higher temperatures in autumn and spring, compared to winter.

Table 3.1. Time-varying conditions of favourability for MPB populations (adapted from Safranyik et al., 1975, and Carroll et al., 2004).

| Condition	Variable	Rationale
P1a	> 305 degree days above 5.5°C, June to end of growing season	Minimum heat requirement from peak flight to egg hatch
P1b	> 833.3 degree days above 0°C, 1 August to 31 July	Minimum heat requirement for population to be univoltine
P2	Temperature below 50% mortality curve	Cold temperature causes mortality
P3	Mean T_{max} in August > 18.3°C	Lower threshold for MPB flight is 18.3 °C
P4	March to June precipitation < normal	Two or more consecutive years with precipitation deficit are related to drought stress and decreased resistance to attack
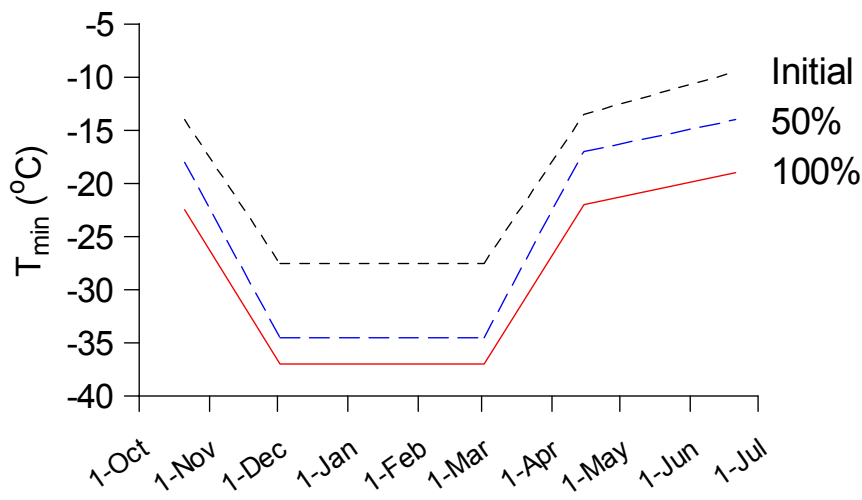
Figure 3.1. MPB Cold mortality curve (adapted from Wygant, 1937).

3.3 *Climatic favourability indices computed from weather station data*

To provide insight into the climatic history of BC as it is relevant for the MPB population, time series of the index components were generated for several stations with long records across BC, including two stations in an area impacted by the most recent outbreak: Quesnel and Barkerville (Figure 3.2). The stations are relatively close together (ca. 50 km) but at different elevations (545 m and 1265 m). The current MPB has recently reached and killed a significant percentage of trees in this area.

In Quesnel, the summer and annual heat accumulations were never a limiting factor, while they were frequently below the favourability thresholds in Barkerville. The frequency of winter days with temperatures below the 50% mortality threshold (P2) clearly decreased over the last few decades. Due to many data gaps at Barkerville, the decrease does not show quite as clearly at this station. Both findings are consistent with the recent warmer-than-normal winters reported for the interior of British Columbia. The August temperatures always exceeded the threshold for flight in Quesnel, but often remained below it in Barkerville. Consecutive years of below-normal early-summer precipitation occurred regularly at both stations, the most recent at the higher-elevation station from 1993 to 1998. While there is high interannual

variability, in general the time series indicate an increasing climatic favourability for MPB. At Barkerville, all conditions were met simultaneously for the first time in 1998.
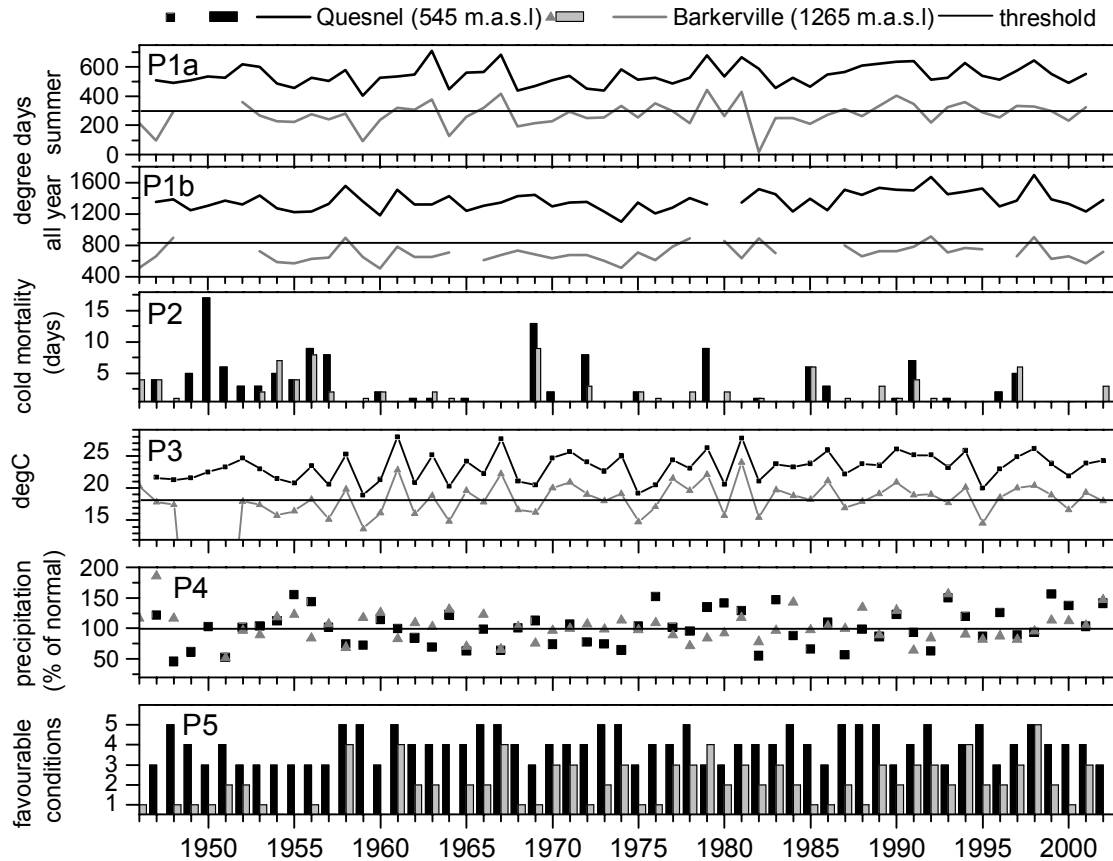

Figure 3.2. Time series of the components of the MPB favourability index for weather stations Quesnel and Barkerville

The comparison of the data from Quesnel Airport and Barkerville, which lies at a higher elevation, illustrates a data-related problem. Most of the weather stations within BC are located in the valleys, close to towns and airports. In those locations, the climatic conditions are favourable for MPB most of the time, at least for summer and annual temperature accumulations, and station data therefore rarely give a representative picture of the conditions up the slopes of the surrounding mountains, where temperatures are lower. As the Barkerville data illustrate, the area is very close to the threshold and a few hundred meters of elevation may change the suitability for MPB immensely. A prerequisite to assessing

interannual climatic favourability in any given location in BC is therefore the ability to extrapolate climate variables accurately for the higher elevations.

In addition to the tendency to decreasing frequency of cold-mortality events, there may have been a change in timing. Figure 3.3 shows dates of cold-mortality events at Quesnel, as inferred from the observed air temperature data and the cold-mortality curves shown in Figure 3.1. Through the 1950s, cold-mortality events occurred as early as late October (~ day 300) and as late as late March (~ day 80). Since then, only two cold-mortality events occurred in October or November (1984 and 1985), with rest occurring from December to February.
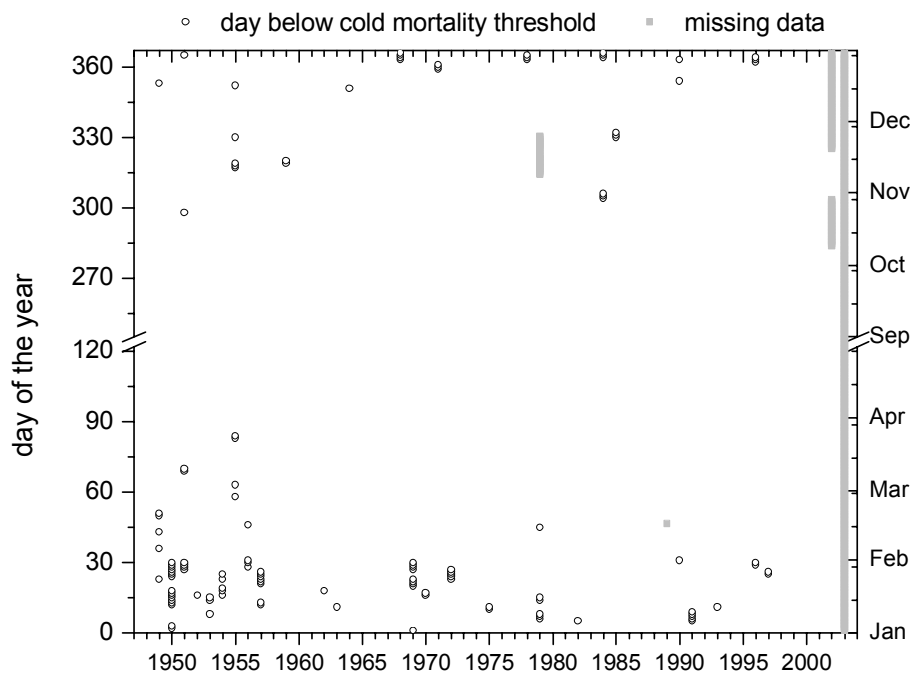

Figure 3.3. Timing of cold mortality days at Quesnel from 1948-2003

3.4   Comparison between climatic favourability indices and outbreak patterns

The climate interpolation model allows the prediction of daily time series of T_{max}, T_{min} and P for any location in B.C., and hence subsequent calculation of the annual climatic favourability indices. Because computing time requirements currently prohibit our ability to interpolate over a grid covering all of BC,

analysis was focused on selected critical regions or historic outbreaks (Figure 3.4): (a) the Chilcotin region, to analyse the climatic favourability for the MPB outbreak from 1973-1985, and (b) three W-E/S-N transects over the Rocky Mountains, in locations of suggested passes that the MPB either have crossed in the recent outbreak (ca. 2000) or are likely to cross in the near future. From north to south these transects are: across Pine Pass to Chetwynd (points P1 to P6), through the Robson Valley over the Yellowhead Pass to Jasper and Pocahontas (J1 to J6), and from the Rocky Mountain Trench over Kicking Horse Pass into Banff and Canmore (B1 to B7).
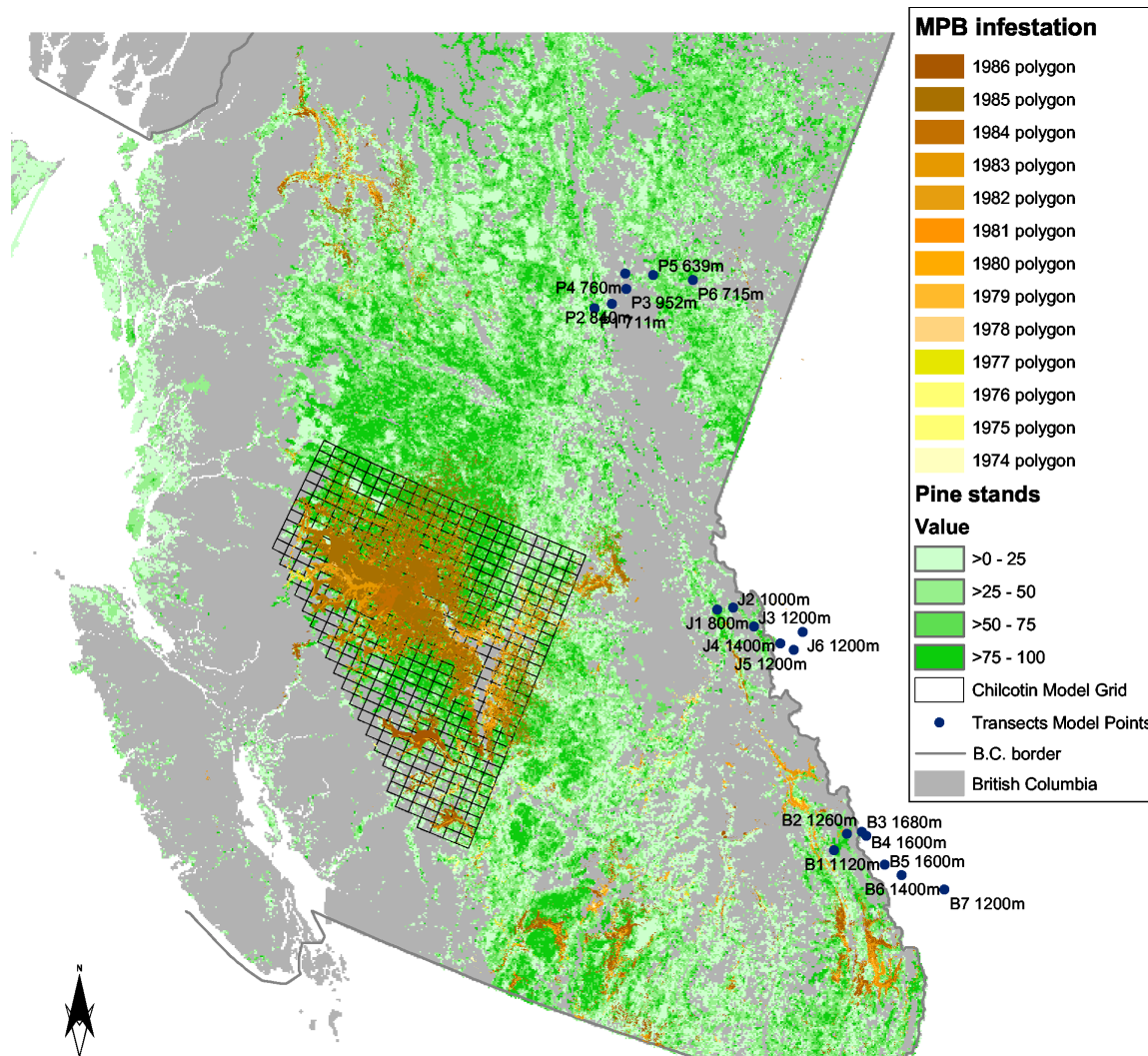

Figure 3.4. Areas of application of the climate interpolation model and derivation of MPB climatic favourability conditions

28

3.4.1 Chilcotin outbreak (1973-1985)

One of the largest outbreaks of MPB before the current outbreak occurred in the late 1970s on the Chilcotin plateau. This outbreak is ideal for testing the contribution of climatic variability because its spatial and temporal dynamics are well documented. The temperature interpolation model was specifically calibrated for the region. The constrained Daymet model was applied with a desirable number of 16 stations, a shape parameter of $\alpha=3.0$, and monthly varying default lapse rates derived from high-low elevation station-pairs in the region. The model was then applied to derive daily time-series for a 469-cell grid with a resolution of 0.2° longitude x 0.1° latitude. The elevations for each grid cell were derived from a 77-m DEM of BC, which for computation time and computer memory purposes had to be resampled to 230-m resolution. The first climate interpolation (CI-1) for the entire study area was performed for the mean elevations for each grid cell. As the grid cells are large and in some areas incorporate significant elevation differences, the interpolations were performed again for the 10th-percentile elevation value of the hypsometric curve of each grid cell (CI-2). For precipitation, only a simple nearest-neighbour interpolation of the annual spring anomalies was conducted. No elevation information was taken into account because the index is based on relative variability, which we assumed would be relatively spatially conservative, rather than absolute variability, which would vary with elevation. From the daily temperature anomaly series and the spring precipitation anomalies, we subsequently derived annual time-series of the five MPB favourability conditions for each grid cell.

The spatial and temporal distribution of the conditions from the CI-1 and CI-2 temperature interpolations for the period 1965-1985 can be viewed as an animation on the project website (www.geog.ubc.ca/~kstahl/mpb/cumconditions.html). Figure 3.5 summarizes the cumulative years during which all favourable conditions were met within the period of 1973 to 1985. The effect of elevation is strong. The spatial distribution of favourable conditions generally matches the infested area in the central part of the study area. However, in the Klinaklini River region, where the infestation started, conditions were only favourable enough to explain the outbreak for the low elevation interpolation (CI-2). The northeast portion of the study area had favourable climatic conditions in a number of years, but the outbreak was stopped in 1985 before fully spreading there. The spread was most likely halted by a cold mortality event in the winter of 1984/1985. However, this area, which was periodically climatically suitable, was recently (in 2003/2004) affected by MPB spreading from the north. The years 1971, 1977 and 1983 were the most climatically favourable within the period, with more than 40% of the grid points favourable for MPB.
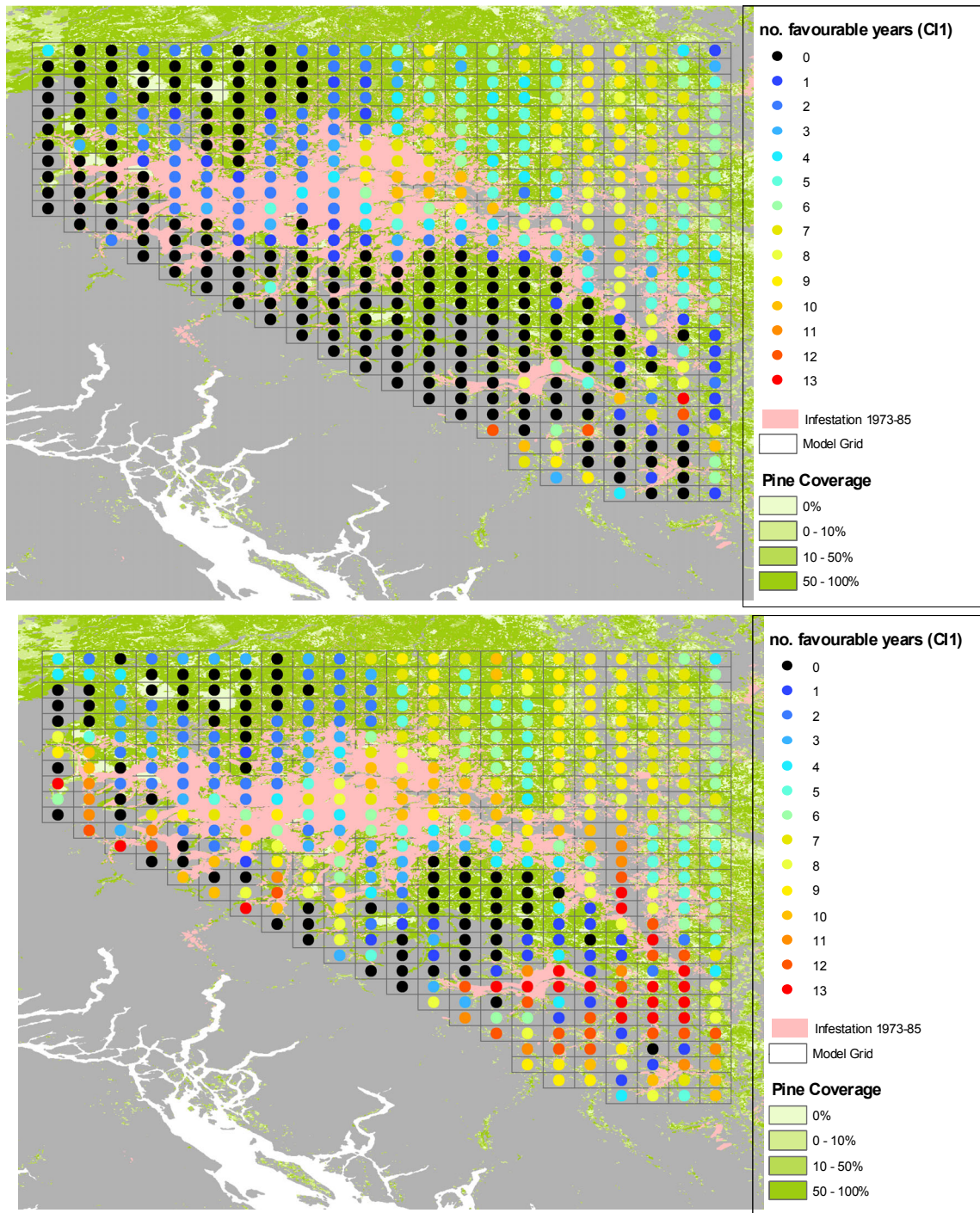
Figure 3.5 Favourable climatic conditions 1965-1985 and MPB infestation in the Chilcotin study area. Upper panel: CI-1 interpolation (mean elevation), lower panel: CI-2 interpolation (10% lowest elevation).
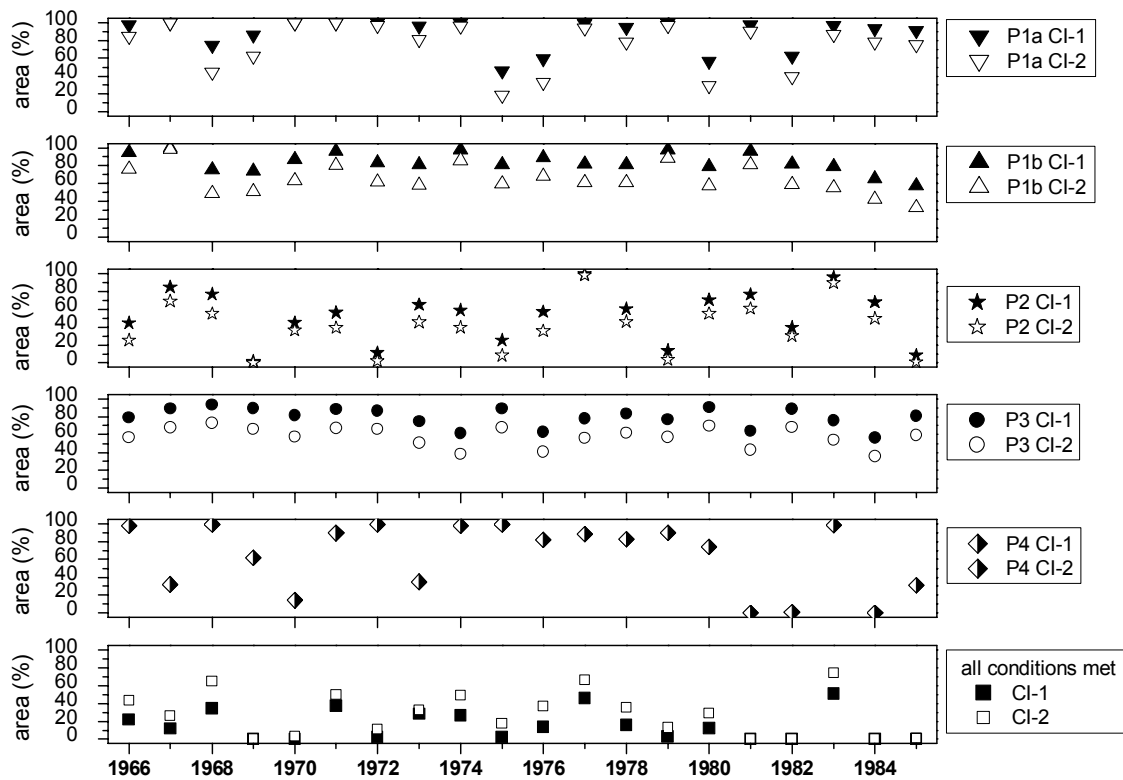
Figure 3.6. Annual percentage of the Chilcotin study area with favourable conditions.

Although Figure 3.5 suggests a reasonable association between lack of infestation and overall lack of climatic favourability, especially using the 10th percentile elevation, it does not reveal whether the interannual variations of the favourability indices are associated with the timing of spread. Tables 3.2 and 3.3 summarize the results of chi-square tests of association, in which each cell-year is treated as an independent observation subject to a two-way classification based on predicted climatic favourability and the occurrence of an increase in infested area. The null hypothesis is that the probability of increased infestation within a cell does not depend on climatic favourability in the previous year (Table 3.2) and the two previous years (Table 3.3). The analysis uses the favourability indices based on the 10th percentile elevations.

Table 3.2. Comparison of occurrence of increased infestation within a cell in relation to whether it experienced favourable climatic conditions over the preceding year. The bottom row shows significance levels for chi-square tests of independence.

	P1a	P1b	P2	P3	P4	P1-3	Pall
Climate not favourable (total)	*1154*	*1589*	*3235*	*959*	*2650*	*3832*	*5080*
No infestation increase (%)	84.0	81.7	79.7	87.8	71.3	79.2	75.0
Infestation increase(%)	16.0	18.3	20.3	12.2	28.7	20.8	25.0
Climate favourable (total)	*5881*	*5446*	*3800*	*6076*	*4385*	*3203*	*1955*
No infestation increase (%)	73.2	73.0	71.0	89.4	77.2	70.0	74.9
Infestation increase(%)	26.8	27.0	29.0	10.6	22.8	30.0	25.1
Significance (p)	<0.001	<0.001	<0.001	0.15	<0.001	<0.001	0.94

Table 3.3. Comparison of occurrence of increased infestation within a cell in relation to whether it experienced favourable climatic conditions over the preceding two years. The bottom row shows significance levels for chi-square tests of independence.

	P1a	P1b	P2	P3	P4	P1-3	Pall
Climate not favourable (total)	*1494*	*2146*	*4499*	*1612*	*3985*	*4499*	*6325*
No infestation increase (%)	83.9	80.2	79.4	88.0	68.6	85.6	75.9
Infestation increase(%)	16.1	19.8	20.6	12.0	31.4	23.5	24.1
Climate favourable (total)	*5541*	*4889*	*2536*	*5423*	*3050*	*2536*	*710*
No infestation increase (%)	72.6	72.7	67.3	89.5	83.4	56.2	66.9
Infestation increase(%)	27.4	27.3	32.7	10.5	16.6	27.7	33.1
Significance (p)	<0.001	<0.001	<0.001	0.10	<0.001	<0.001	<0.001

In both cases, criterion P3 (based on August maximum temperatures as a condition for flight) does not show a significant association with the occurrence of an increase in infested area within a grid cell. Criterion P4 (less-than-normal spring precipitation) does show a statistically significant association, but it is in the opposite direction to what would be expected. For the case of the preceding 2 years, there is a higher probability of infestation increase for unfavourable conditions (31.4% compared to 16.6%).

The two heat accumulation indices and the winter cold mortality criterion are all significantly associated with increased infestation. For all three indices, the occurrence of increased infestation occurred about 50 to 100% more frequently in cells that had climatically favourable conditions compared to those with unfavourable conditions. For example, considering the two preceding years, 27.4% of the cells with favourable conditions exhibited an increase in infestation, compared to 16.1% of those with unfavourable

conditions. These results indicate that the climatic favourability indices have predictive skill, but are not fully reliable predictors of unfavourable conditions.

The aggregate index (Pall) exhibits no predictive skill when it is based only on the preceding year. However, it exhibits significant skill when the two preceding years are considered.

The results in Tables 3.2 and 3.3 must be interpreted cautiously, because the assumption that cell-years represent independent observations is likely not valid. The analysis does not account for spatial correlation in the underlying conditions within the cells that may influence the probability of infestation (e.g., stand conditions) or in the climate interpolation errors (e.g., if the annual heat accumulation is overpredicted in one cell, it is likely over-predicted in neighbouring cells). An important factor ignored by this analysis is the influence of infestation in neighbouring cells. More complex statistical analyses are being conducted by Brian Aukema and co-workers at the University of Wisconsin to incorporate influences of spatial and temporal dependence.

3.4.2   Pine Pass transect

On the infestation maps, there were small affected areas west of Pine Pass in 1999 and 2000. The first to appear east of the pass, in 2000, was fairly isolated near Chetwynd. In 2002, the patches west of the pass grew larger and by 2003 they expanded into higher altitudes south of Pine Pass. In 2004, traces of red attack were mapped between P2 and P3 and between P4 and P5 in the Pine Valley. Furthermore, there were major infested areas in the valleys to the south. The results of the climatic favourability calculations for this transect are shown in Figure 3.7. On both sides of the pass the climate seemed generally suitable for MPB. If any condition was limiting, it was P2, the cold mortality condition. All other conditions were met frequently. On the pass, P1a/b and P3 have been met less regularly, but still far more often than P2, although P2 was met for three consecutive years from 1999 to 2001 at all points. However, MPB likely crossed the northern Rockies by long-distance aerial dispersal rather than by ground-based spread, thus minimizing the ability of climatic conditions at Pine Pass to control their movement into northeast BC (A. Carroll, Canadian Forest Service, pers. comm.).

Figure 3.7. Annual history of favourable climatic conditions for MPB along the Pine Pass transect

3.4.3 Jasper transect

The Robson valley on the west side of the Yellowhead Pass, which crosses the Rockies into Jasper, has come under MPB attack in recent years. On the infestation maps, the first outbreaks appeared in 2000 near point J2. They expanded in 2001, and in 2002 an affected area appeared just past J3. In 2003 the affected areas between J1 and J2 expanded and did so again in 2004, when the area below J3 was also affected. The climatic favourability time series for this transect are shown in Figure 3.8. On the west side of the pass climate was apparently not limiting MPB population expansion, except for condition P2 in some years. However, the frequency of condition P2 (no cold mortality) appears to have increased gradually over the time period analyzed and points J1 to J3 also show a series of 4-5 years of no cold mortality starting in 1999. Yellowhead Pass appeared to be a climatic barrier to MPB, but not a particularly consistent one, as all conditions have been met frequently, and a synchronous timing in the future may be likely if current trends to warmer winters continue. On the east side of the Pass, the cold

mortality again was the limiting factor. A trend to more frequent "warm" winters is not as pronounced as for the western points on the transect.
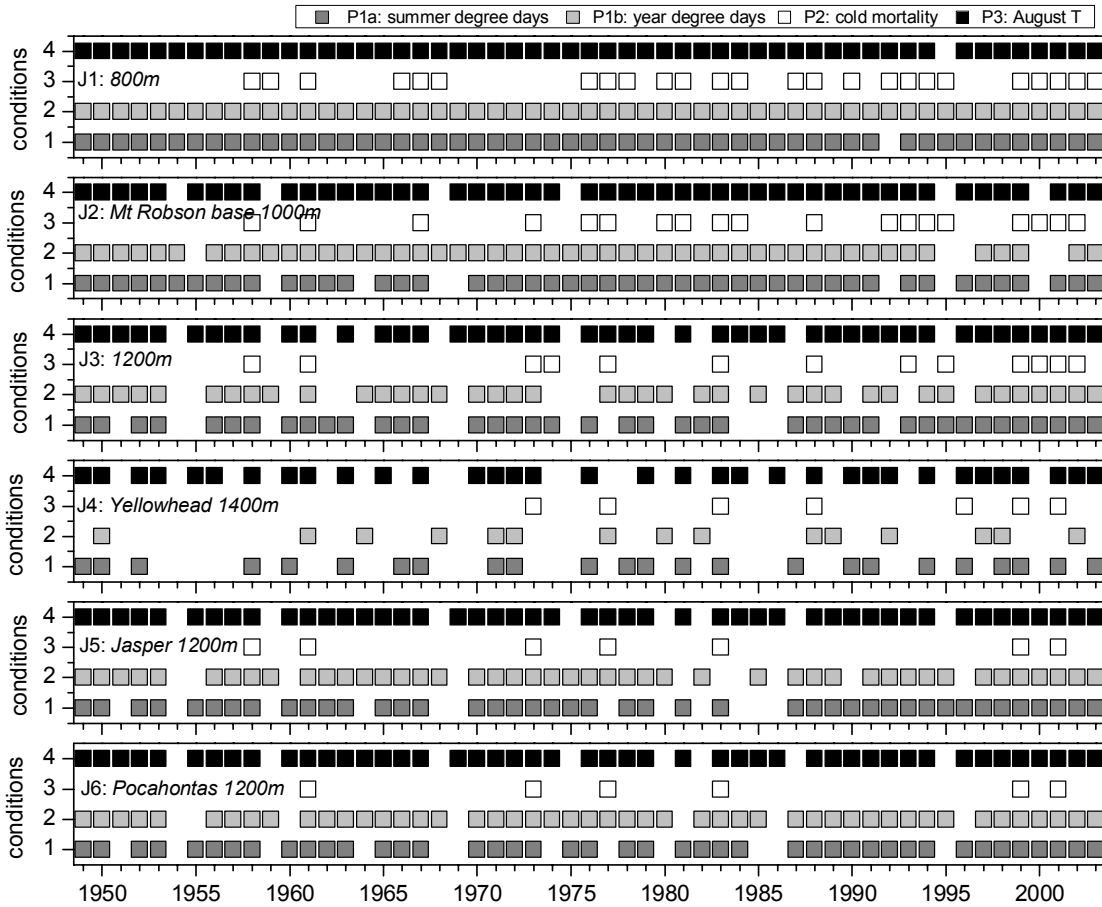

Figure 3.8. Annual history of favourable climatic conditions for MPB along the Jasper transect

3.4.4   Banff transect

Similarly to the Jasper transect, the west side of the southernmost transect across Kicking Horse Pass into Lake Louise and Banff also showed the first signs of MPB infestation in 1999 and 2000. The infested areas expanded and in 2001 a patch appeared close to point B1. The affected area in the Rocky Mountain Trench expanded further in 2003, yet only small patches were affected beyond B1. While the affected area expanded further in 2003 and 2004, the MPB did not spread much beyond B1 on the British Columbia side. However, MPB have established near Banff and Canmore (Alberta Government, 2005).

Figure 3.9 shows the climatic favourability indices. As in the previous examples, the limiting condition in the lower elevations was P2. However, since 1999, it was met every year at point B1, and at B2 it was met in 2000, 2001 and 2003. Kicking Horse Pass and the area immediately east into the Bow Valley seemed to provide an effective climatic barrier. However, the indices suggest that favourable conditions have recently prevailed at Canmore, consistent with the observations of MPB establishment.

Figure 3.9. Annual history of favourable climatic conditions for MPB along the Banff transect

3.4.5   Evaluation of the climatic favourability indices

The time series of the climatic favourability indices are broadly consistent with observed outbeak patterns in time and space, although the apparent crossing of MPB into Banff and Canmore is inconsistent with

36

the index values at Kicking Horse Pass, which suggest that summer heat accumulation should be a limiting factor. However, these comparisons cannot be considered a critical test of the indices, as it is difficult to account for lag effects in MPB population dynamics without coupling the climate-based indices to spatially explicit models describing MPB life history and spread. Given these problems with evaluating the climatic favourability models on the basis of MPB outbreak data, it is useful to consider the sources of uncertainty in their calculation, which fall into three main categories: (1) the threshold values used to define them (e.g., the thresholds for cold mortality shown in Figure. 3.1); (2) errors in the interpolation routine; and (3) the representativeness of interpolated values in relation to site-scale microclimatic variability.

Uncertainty in the threshold values can be addressed by continuing experimental and observational studies of MPB life history and sensitivity to climatic conditions. One particular issue is that thresholds may vary regionally, such that cold-mortality thresholds defined for southern populations may not be applicable to populations in northern BC.

Errors in the interpolation routine can be sizable, particularly when extrapolating to high elevation or for interpolating in regions with sparse station coverage. The former problem is ameliorated to some extent in more recent years due to the availability of higher-elevation data in the Snow Pillow and Fire Weather networks. An area of particular concern is the interpolation of minimum daily temperatures (which are subject to greater uncertainty than daily maximum temperatures), due to the apparent importance of winter cold mortality as a control on favourability for MPB.

The data that form the basis for interpolations are measured at climate stations, which are generally located at level sites in openings. Thus, they may not represent conditions on slopes, particularly in situations where radiative heating or cooling vary strongly with aspect. Furthermore, the station data may not be representative of conditions under a forest canopy. A related issue is that temperature conditions within the bark may differ from air temperature due to time lags associated with heat conduction, particularly where a snow pack covers the lower portions of the trunk. Thus, even where the indices suggest regionally unfavourable climatic conditions, there may be habitats within the region that are favourable.

3.5 Links to large-scale climatic phenomena

As shown in the previous section, the interannual variability of favourable climate for MPB in critical regions in BC appears to be dominantly limited by the winter cold-mortality condition, and additionally by summer heat accumulation at higher elevations in the Rocky and Columbia Mountains. In this section, the analysis concentrates on the links between larger-scale atmosphere-ocean conditions and winter temperatures. It begins by examining the linkages between potential cold-mortality events and synoptic-scale circulation patterns, then shifts to the role of larger-scale phenomena such as ENSO and PDO.

3.5.1 Relations between cold mortality events and synoptic-scale circulation patterns

Days with temperatures below the 50% cold mortality threshold at the selected weather stations are associated with several circulation types (Figure 3.10), of which type 6 is the most frequent throughout BC. The MSLP pattern of this type indicates an "Arctic Outbreak" situation, with cold Arctic air flow into BC from the northeast causing low temperatures across the province. In northern BC, types 2, 3, and 10 also frequently produce temperatures below the mortality threshold. The isobars of types 3 and 10 indicate northeasterly flow of Arctic air into northern BC. Types 2 and 5 are additional important cold-weather situations in central BC. Type 2 represents generally high pressure over the Pacific and type 5 is characterized by a continental ridge reaching into interior BC from the south. In southern BC, where cold mortality days are generally rare, type 11 plays a role. This type has a somewhat weaker ridge over the interior.

3.5.2 Relations between cold mortality events and large-scale climate indices

Visual examination of the climatic favourability histories for the three transects suggests that the frequency of favourable winter conditions was greater for the period from 1977 to 2003 than for the earlier period. Such a change would be consistent with the well-documented 1977 climate shift that involved a tendency to greater dominance of the enhanced phase of the PNA pattern and the neutral and positive phases of PDO, which are associated with warmer winters in BC, as demonstrated in section 2 and by Moore and McKendry (1996). The research hypothesis that the frequency of favourable winters (i.e., no cold mortality events) has been greater since the 1977 climate shift was tested using a chi-square test of independence (using pre-shift/post-shift and favourable/unfavourable as contingency table categories). The null hypothesis is that the probability of a winter being favourable is the same both before and after the shift. As seen in Table 3.4, the null hypothesis can be rejected for four of the sites on

the Pine Pass transect, three on the Jasper transect, and none on the Banff transect. At Pine Pass, significant changes occurred at the higher elevation sites, while at Jasper the significant changes occurred at the western sites. Given the exploratory nature of this analysis, we chose not to apply a Bonferroni or other correction for multiple comparison.
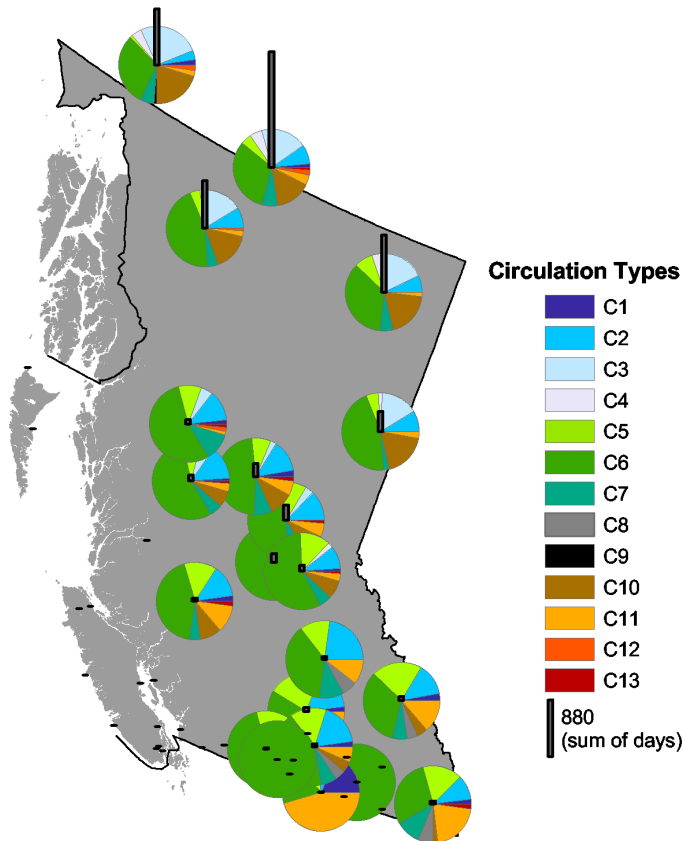

Figure 3.10. Number of cold mortality days 1948-2003 and distribution of circulation types associated with cold mortality days.

Table 3.4. Results of chi-square tests for a change in frequency of favourable winters before and after the 1977 climate shift. There were 28 years pre-shift and 27 years post-shift. The p-values are the probabilities of a greater value of χ^2 if the null hypothesis were true.

Transect	Site Elevation (m)	# favourable years (pre shift)	#favourable years (post shift)	χ^2	p
Pine Pass	711	4	8	1.90	0.17
	840	1	9	8.18	0.00
	952	1	9	8.18	0.00
	760	3	9	4.12	0.04
	639	4	8	1.90	0.17
	753	1	7	5.53	0.02
Jasper	800	7	18	9.63	0.00
	1000	5	14	7.03	0.01
	1200	4	9	2.76	0.10
	1400	1	6	4.30	0.04
	1200	3	4	0.21	0.65
	1200	2	4	0.83	0.36
Banff	1120	10	16	3.06	0.08
	1260	8	9	0.15	0.70
	1680	2	4	0.83	0.36
	1600	2	5	1.60	0.21
	1600	1	4	2.10	0.15
	1400	2	4	0.83	0.36
	1200	6	12	3.31	0.07

The chi-square tests suggest that some locations have had a decreased frequency of winter cold mortality since the 1977 climate shift to an increased dominance of the neutral and positive phases of PDO. This change in cold-mortality frequency is broadly consistent with the tendency to higher mean winter temperatures during neutral and positive phases of PDO, and also with the associated tendency to fewer days with synoptic types associated with cold-mortality conditions. However, the link is not so clear on an interannual time scale, as the negative PDO conditions in 2000 (Figure 2.8) were apparently associated with no cold-mortality events (Figures 3.2, 3.7-3.9).

Further analysis examined the hypothesis that the probability of cold-mortality events, for a given synoptic type, differed among the PDO phases. Using a chi-square test of independence, statistically significant ($p<0.05$) differences in cold-mortality day frequencies were found for Types 2, 3, 6, and 10 (Fort St. John) and Types 2, 5, 6, and 11 (Prince George and Quesnel). Figure 3.11 shows these frequencies, which were all considerably higher during negative PDO winters than during neutral and positive phases. The differences between the phases increased from north to south, suggesting a weakening of the signal toward northeast BC. However, the frequencies of cold mortality days at stations in southern BC were too low to allow a statistical test. The same test for different ENSO phases showed no significant differences at the three stations.
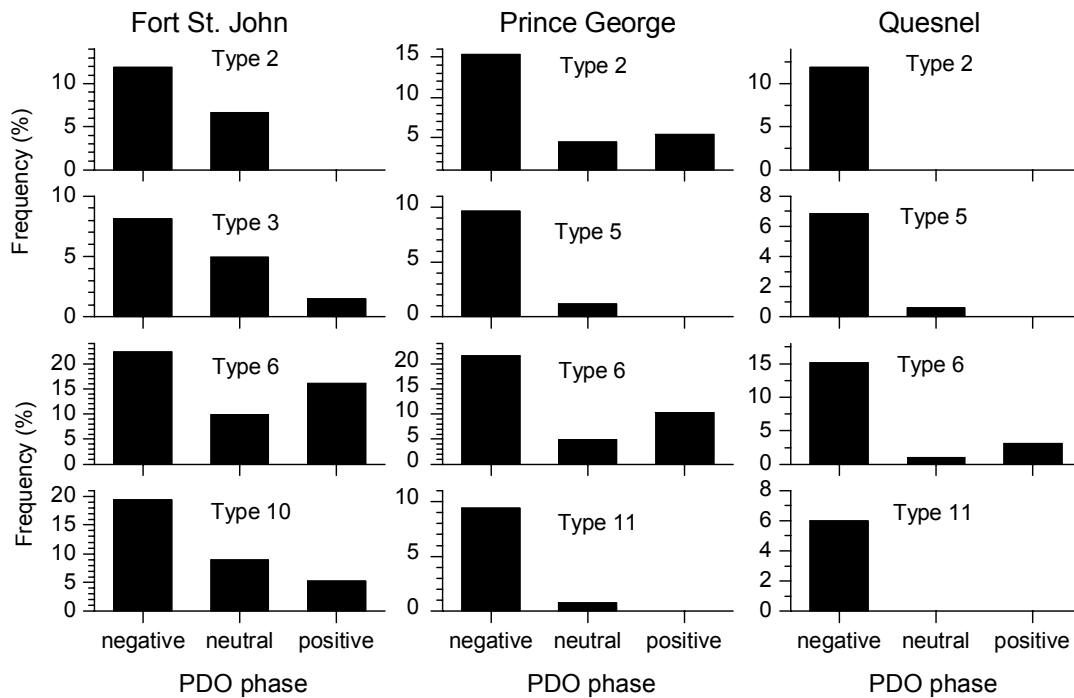
Figure 3.11. Frequency of cold mortality days at three stations in 1948-2003 for selected circulation types during different phases of the PDO.

These analyses indicate that cold-mortality days occurred more frequently during negative PDO winters than during a neutral or positive PDO phase winter. The cause was a combination of more occurrences of the anticyclonic synoptic types 2, 3, and 6 as well as a higher chance for extremely cold days within types 2, 3, 5, 6 and 11. Type 6, the Arctic outbreak, had the largest net effect on the occurrence of cold mortality days in this respect. However, the recent run of favourable winters beginning in 1999 included

41

both negative and positive PDO phases, suggesting that there may be other factors that can modify or even confound the apparent teleconnection between PDO phases and occurrence of cold-mortality conditions. This issue deserves further study.

3.6   Scenarios for future MPB activity

The analyses described above suggest that climatic conditions have become more favourable for MPB spread since the 1970s and have contributed to both the Chilcotin outbreak that ended in 1985 and the most recent outbreak beginning in the late 1990s. In particular, the apparent tendency to less frequent cold mortality in winter is consistent with the known effects of the 1977 climate shift on temperatures in BC. An important question is whether these milder winter conditions will persist, producing a long-term expansion of suitable MPB habitat in BC and into the boreal forest, or whether a future shift may produce a climatic regime with colder winters (as occurred in the 1947 PDO shift).

An original goal of this study was to examine this question using two approaches: (1) by applying the climatic suitability indices based on daily climate data to future climatic scenarios generated by General Circulation Models (GCMs), and (2) by using synoptic-scale patterns predicted by GCMs to examine how the frequencies of cold-mortality synoptic circulation types might change in the future, thus providing an indirect index of winter climatic favourability. However, we were unable to obtain suitable scenarios with a daily resolution, which would be required to apply these approaches. Most scenario output appears to be available at monthly resolution, which would require some sort of temporal downscaling to generate daily values. An approach employing temporal downscaling has already been applied by Carroll et al. (2004) and thus was not conducted as part of the current study. Carroll et al. (2004) found that future climatic scenarios indicate an expansion of MPB suitability through to the year 2060.

4 Stand-scale influences

4.1 Introduction

Landscape effects of climate change result from a combination of stand-level ecosystem processes and dynamics, and landscape-level natural disturbance effects. An analogy can be drawn between climate change effects on stand-level forests and "ecological theatre". Climate, soil, topography, geology and natural disturbance effects set the "ecological stage". This determines which "ecological plays" (sequences of biotic communities that successively occupy and are replaced by other communities on a site following disturbance) can occur on a particular part of the landscape. The "ecological play" in turn determines which "ecological actors" (species) are present during the different "acts" (seral stages) of the "play" (the ecological succession, or sere). Predicting future "ecological plays" requires an understanding of how the "ecological stage" (e.g. climate) may change in the future, and how this will affect the "ecological play" and "actors". Understanding and predicting these effects requires an understanding of stand-level ecosystem processes.

As a consequence of the important role that stand-level processes play in determining landscape-level response to climate change, including the risk and consequences of mountain pine beetle epidemics, landscape-level models of climate change effects and related landscape-scale natural disturbances events should be linked to, and driven by, climate-sensitive, stand-level, ecosystem management models. The majority of stand level forest models are either: 1) "historical bioassay" (HB), experience based statistical models. These are usually regression models fitted to empirical data on how stands have grown in the past with one or more of time, tree height, tree diameter or similar mensurational measures as the independent variable(s). Such models simply project the record of past growth into the future and are unable to address changed futures, such as forest development under climate change; or 2) population-level or tree community-level models based on competition for light. Neither of these categories of model is suitable as a driver of landscape-level models in which future forest growth and development, and the risk and character of future natural disturbances depend on many factors that are changed from the past.

In response to the need to drive landscape-level disturbance and climate change response models with climate sensitive, stand level, ecosystem management models, we are modifying the FORECAST model to give it climate change capability and the ability to link to mountain pine beetle risk models, fire risk and severity models, and to wildlife habitat suitability models. Providing climate sensitivity involves adding a water balance and soil moisture model (ForWaDy) to FORECAST. The modified model can

then be linked to a landscape-level model such as ATLAS (other models such as SELES would also be suitable) (Figure 4.1).

FORECAST (FORest Ecosystem Change ASsessmenT; Kimmins et al., 1999) is a hybrid simulation, non-spatial, stand level, ecosystem management simulator. It is a hybrid model since it combines output from well documented HB models with our current understanding of key ecosystem processes to produce a process-based simulation model that is much easier to calibrate than traditional process models. The output from the HB models represent the measured result of a variety of ecosystem processes. By combining this output with our understanding of ecosystems, we are able to infer the rate of several key ecological processes. These estimates are then used to calibrate the process model ECOSYTSM (Figure 4.2) rather than having to undertake the lengthy, difficult and expensive field measurement of these processes. Literature data or limited field sampling can generally be relied on to provide other data that cannot be obtained in this manner. Figure 4.3 lists the major management interventions that can be made in FORECAST.
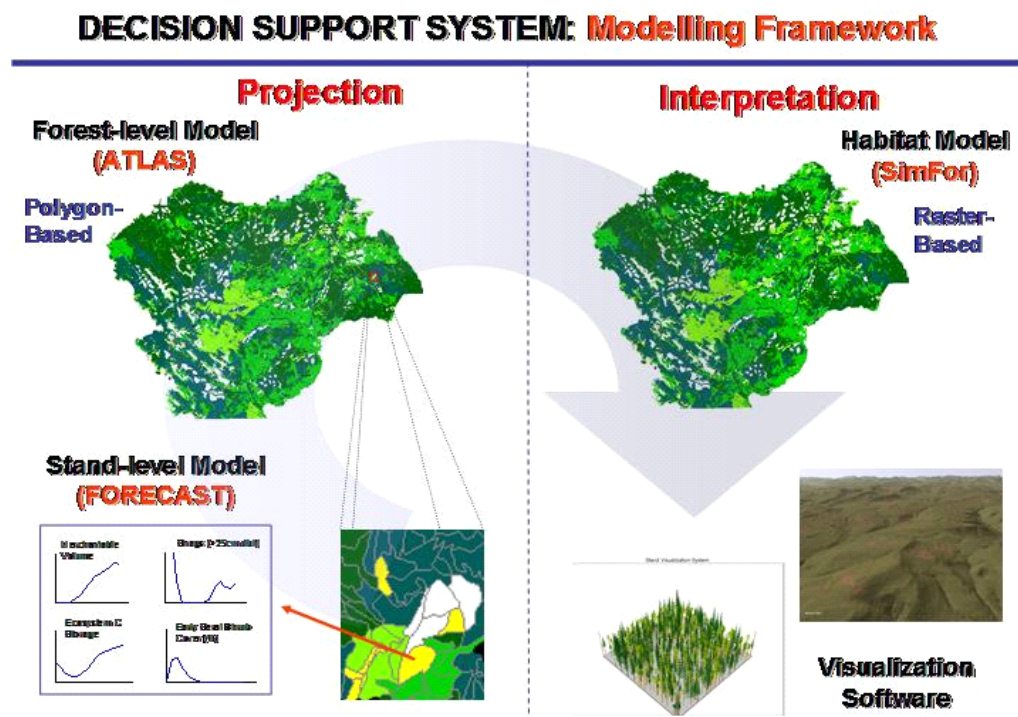
Figure 4.1. Linkage of FORECAST – a stand-level, ecosystem management simulator – to the landscape-level timber supply model ATLAS, and to the wildlife habitat suitability model SIMFOR and visualization software (Seely et al. 2004)
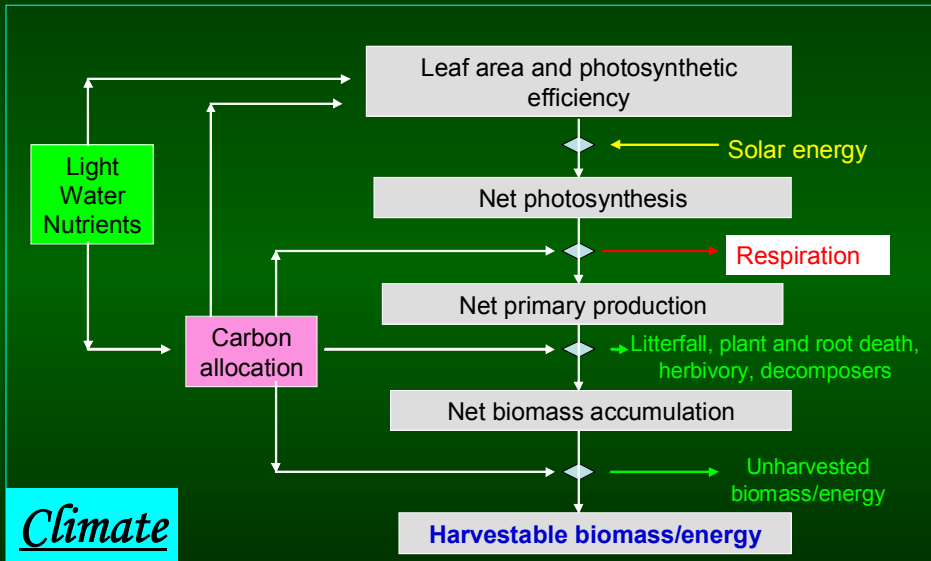
44

Figure 4.2. Flow chart of the key processes represented in FORECAST. Sub-models determine available light, nutrients and soil moisture (Kimmins et al. 1999). All of these are affected by the climate submodel.

Figure 4.3. Management interventions that can be simulated in FORECAST.

ForWaDy is an energy-balance water budget model developed by Seely et al. (1997) (Figure 4.4). It has been successfully linked to FORECAST as a part of this project, and validation projects have been conducted in three different field locations.
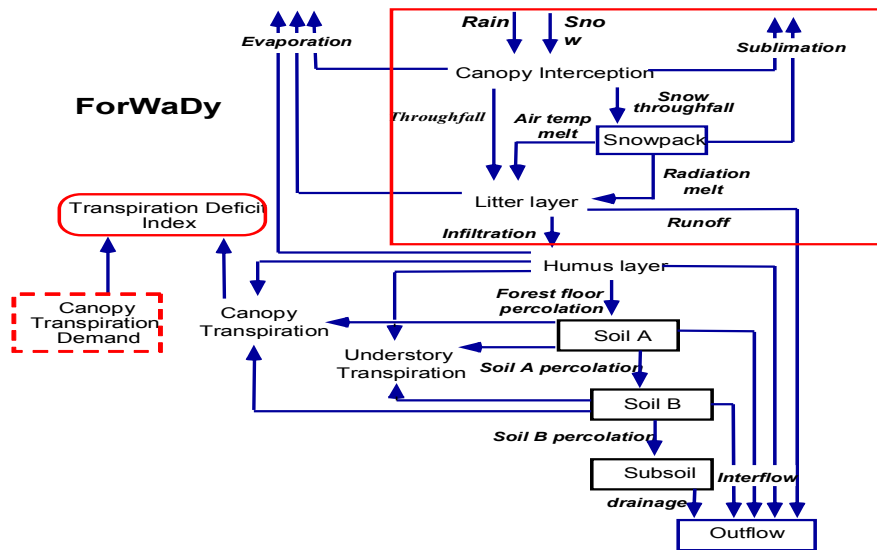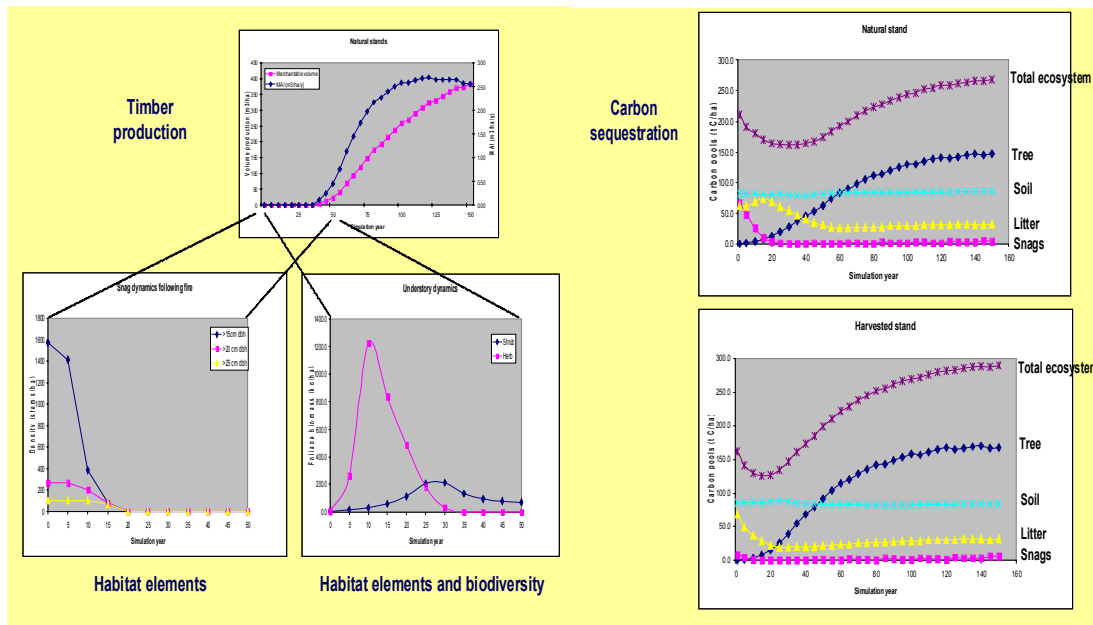

Figure 4.4. Flow chart of the ForWaDy model.

Figure 4.5. Some examples of the abundant output from FORECAST for a lodgepole pine ecosystem in southern B.C.

46

4.2 Climate change strategy in FORECAST

Modifications to the FORECAST software that have been made in association with this project (these were all funded by alternative sources since the requested funds for this were not awarded) include the following:

1. Soil processes. Decomposition is now affected by input data on temperature, and simulated soil moisture produced by ForWaDy. Annual decomposition data that are part of the FORECAST input data set are disaggregated into daily decomposition rates using temperature-decomposition and moisture-decomposition relationships from the literature in combination with weather data from the past 30 years, so that the effects of seasonal variations in future climates (from climate change model scenarios) on this aspect of ecosystem function can be presented.

2. Plant processes. Plant growth in FORECAST (trees, shrubs, herbs, bryophytes – the user can select to simulate any one or any combination of these life forms) is driven by simulated photosynthesis as a function of foliage mass, foliar nitrogen content, and moisture stress effects. Photosynthesis is related to temperature (input data) and soil moisture (ForWaDy simulation) and the feedback effects of plant nutrition (simulated nutrient cycling, which is affected by temperature and moisture). Estimates of annual photosynthesis produced by FORECAST are disaggregated into daily rates using photosynthesis-temperature and photosynthesis-moisture relationships from the literature. This gives the model considerable sensitivity to respond to input data on future climate change scenarios. Length of growing season and growing season frost event effects are to be added in the future.

3. Climate change effects on fire risk and severity. The fire sub-model that is being developed will allow a simulation of changed fire risk and severity as a function of climate change and other natural disturbance events (e.g. mountain pine beetle) that affect fuel loadings.

4. Stand-level mountain pine beetle risk will be simulated by linking FORECAST with existing MPB risk models that relate to stand structure, age, tree size and climatic conditions.

5. Stand dynamics and succession in response to climate change effects and natural disturbance are simulated as described, and as a result of simulated tree growth, competition and natural disturbance. The effects of this on wildlife are represented in terms of wildlife habitat suitability modeling.

4.3   Test of Climate-FORECAST

All models require testing (validation, utility, cost-effectiveness and other measures) before they can be used with confidence in decision-support systems. Testing models that forecast over long time scales and large spatial scales is problematic, which is one reason why FORECAST is equipped with such abundant output – it gives many measures by which its performance can be assessed.

We decided to test Climate-FORECAST against tree-ring measures of climate-related tree growth on Tree Farm License 49 (Tolko, previously Riverside) just east and northeast of Kelowna in the southern interior of B.C. Two approaches are being used:

1. Data on tree ring variation in width, earlywood-latewood ratios and total ring density are being gathered and compared with historical climatic data for the area. This is a study of variation in time – a temporal gradient of climate. Two problems are faced in this approach. Firstly there are almost no climatic data for the areas of the mountain pine beetle outbreak in the study area (mid to upper elevations, the Montane Spruce Biogeoclimatic Zone). Secondly, tree ring variation in response to climate is best expressed on moisture-stressed sites . On the rolling plateau of TFL 47 Montane Spruce zone, there are relatively few very dry forested sites. The samples were taken from mesic sites because in most cases these were the only sites available.

2. Data are being collected on variation in tree ring characteristics with increasing elevation, which represent a climatic gradient – a spatial gradient of climate. Tree cores have been obtained along two elevational sequences. A third may be sampled if funding is obtained (Figure 4.5). There are no tree species than span from low to the highest treed elevations in TFL 47, so three species were selected for study – Douglas-fir, interior spruce, and lodgepole pine. A problem with this approach is that there will be elevational ecotypes within these species – genetic sub-populations adapted to different climates. However, the climatic gradient is sufficiently steep that an overall climate-growth relationship is expected. The alternative of studying a N-S climatic gradient poses other problems, including variations in day length. For practical reasons, the elevational gradient was selected.
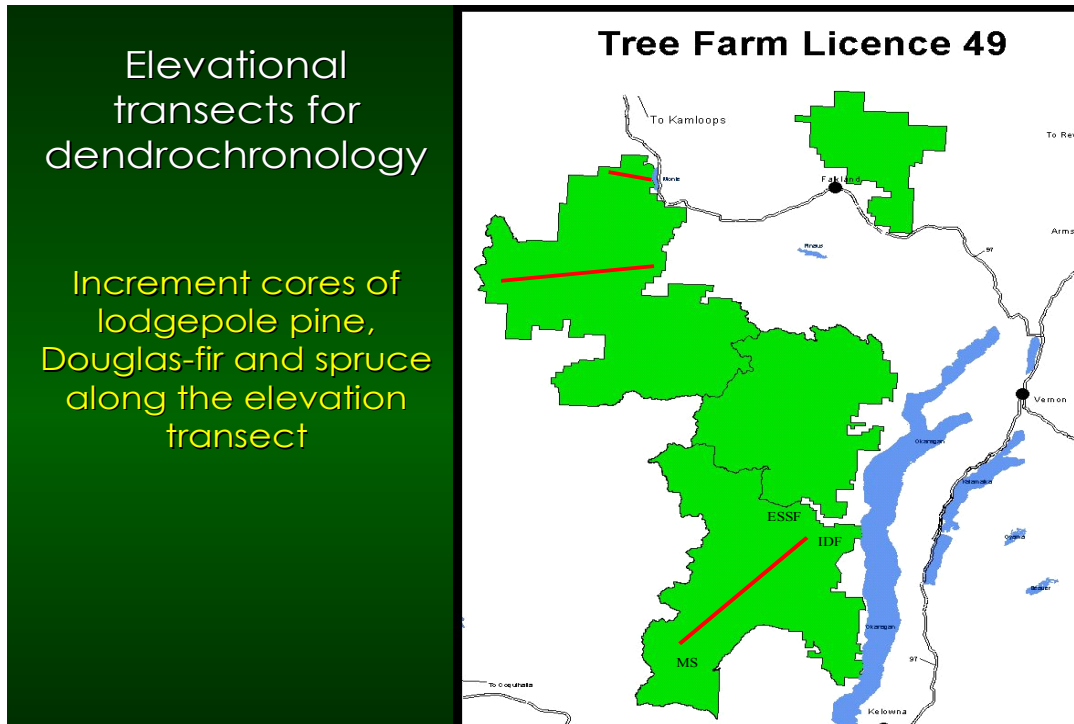
Figure 4.5. Location of elevational sequences of study sites for tree coring. TFL 49.
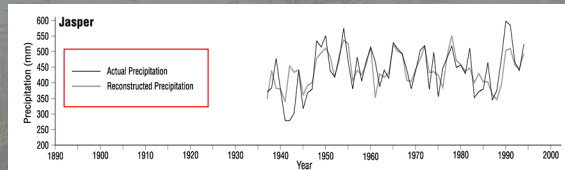
Figure 4.6 shows the overall approach used in this dendrochronological approach. To address the lack of climatic data for the study sites, we used a combination of ClimGen to summarize past climatic data sets for low elevation climatic stations in the study area and to project future climatic regimes, and MTCLIM to extrapolate from these low elevation stations to the elevations of the study sites. We validated these MTCLIM extrapolations against ski area and a mine site's climatic records from high elevation. Figure 4.7 shows the location of the low elevation stations used with ClimGen, and the high elevation ski areas/mine site. Figures 4.8 - 4.9 present comparisons between ClimGen predictions of future climates, assuming no climate change, and the historical data sets for Hedley for precipitation and min. temperature. Figures 4.10 – 4.11 show simulated precipitation and min. temperatures for Hedley mine (high elevation) using MTCLIM and the real data for that site. Statistical comparisons between predicted and actual data showed differences that are being explored and are believed to be a function of the temperature interval used in the analysis. The comparisons are to be re-done for only the range of temperature that has ecological significance.

49
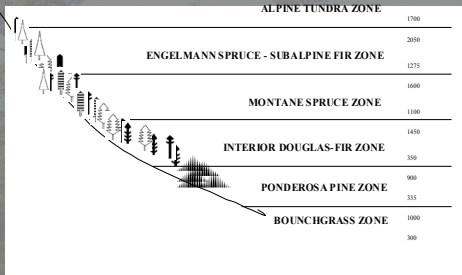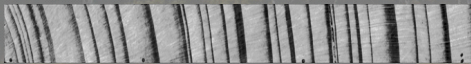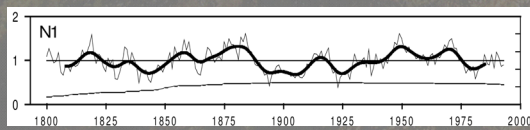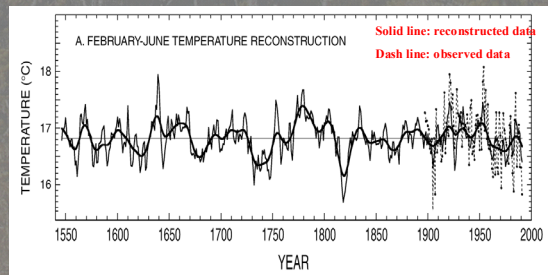
Figure 4.6. Overall approach used in the validation study

Station	Code	Latitude	Longitude	Elevation (m)	Record year
HEDLEY	1123360	49.357	–120.077	517	1904–2002
HEDLEY NP MINE	1123390	49.369	–120.022	1,707	1904–2002
APEX MTN LODGE	1120447	49.400	–119.917	1,889.8	1965–1971
VERNON NORTH	1128583	50.344	–119.271	512	1990–2002
VERNON SILVER STAR LODGE	1128584	50.358	–119.056	1,572	1970–2002
ADRA	1120090	49.733	–119.583	1,002.5	1928–1953
BIG WHITE	1130874	49.733	–118.933	1,841	1981–1999
BIG WHITE MTN LODGE	1130875	49.733	–118.933	1,844	1965–1968
PEACHLAND MINOS ROCK	1126071	49.783	–119.715	351	1973–1981

Figure 4.7. Details of weather stations used in testing ClimGen and MTCLIM; southern interior B.C.
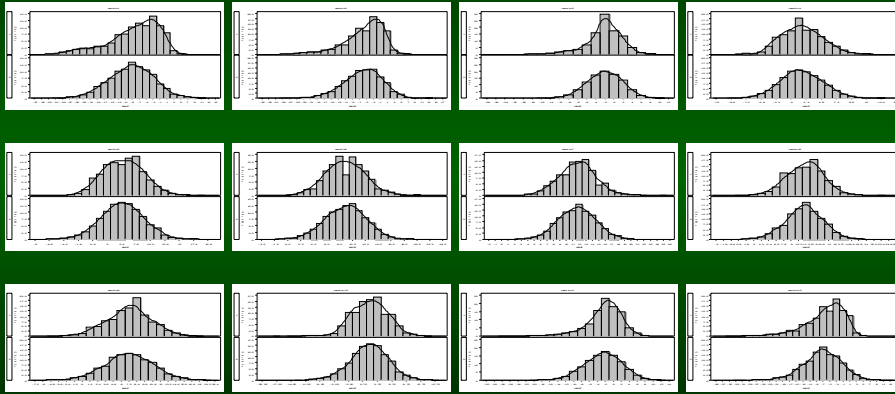
Figure 4.8. Frequency distributions for minimum temperature classes, Hedley climate station using ClimGen
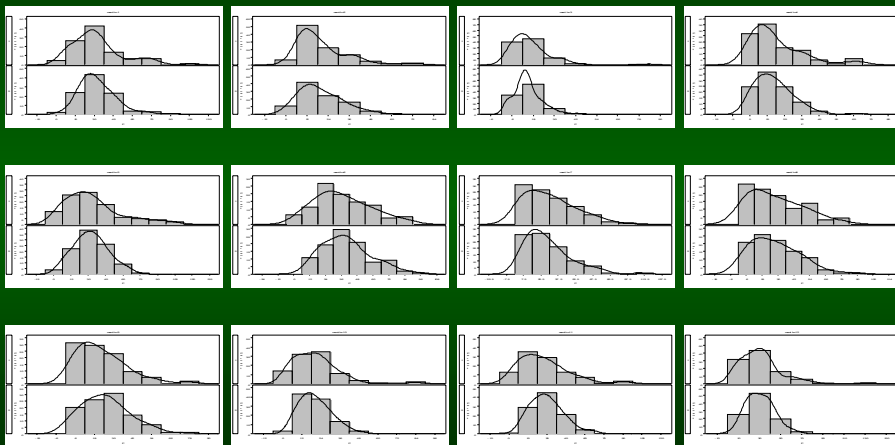
Figure 4.9. Frequency distributions for precipitation classes, Hedley climate station using ClimGen

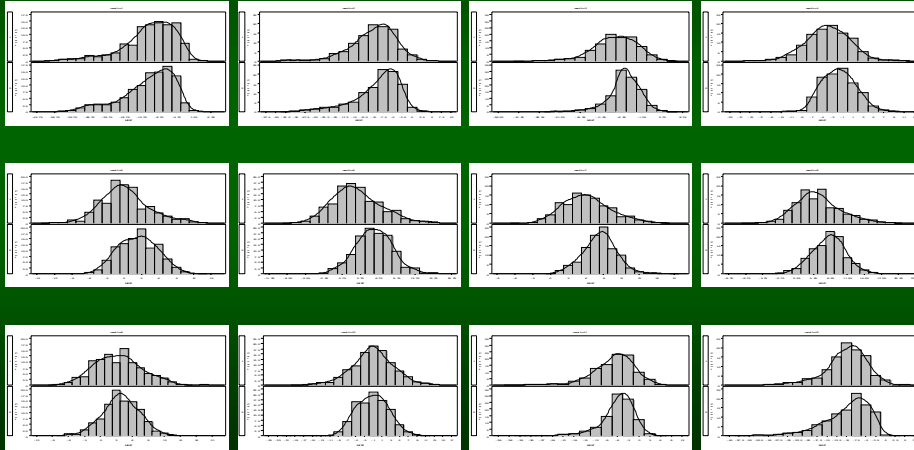**Figure 4.10.** Frequency distributions for min. temperature classes simulated for Hedley mine by MTCLIM from ClimGen output.
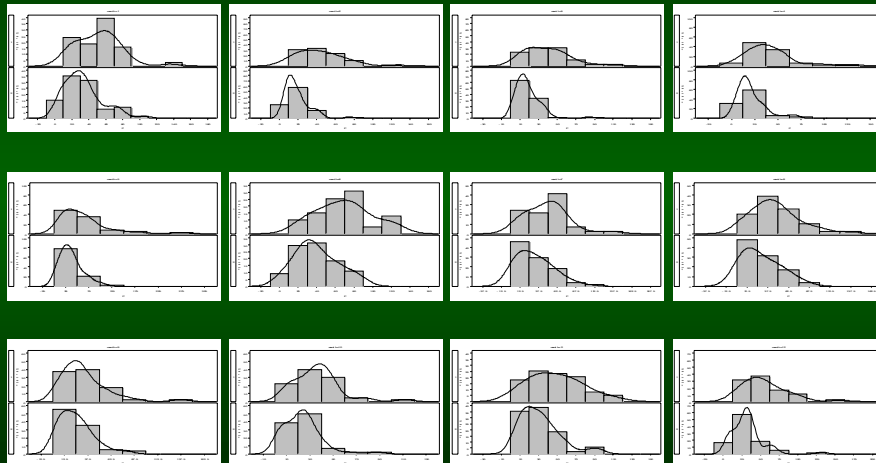

Figure 4.11. Frequency distributions for precipitation classes simulated for Hedley mine by MTCLIM from ClimGen output.

Thus, the strategy for testing Climate-FORECAST is: 1.Generate elevation and temporal climate data sets using MTCLIM and ClimGen; 2. Establish tree growth trends over time and across the elevation climatic gradient by dendrochronology. 3. Predict tree growth over time and along the climatic gradient using Climate-FORECAST. 4. Compare Climate-FORECAST predictions with dendrochronological data.

Progress on the project was limited by lack of funding to accelerate software development, by difficulties in field data collection, including the problem that some of the early data collected were lost when a student's bag was stolen, delays in processing the tree cores, and inadequate funding. Nevertheless, progress has been made and it is anticipated this aspect of the project – development of Climate-FORECAST and its test against the tree ring data - will be completed by the end of 2005.

4.4   Details of the field work

The experimental site is located in Tolko's (formerly Riverside's) Tree Farm License 49 (TFL49), which is in the Okanagan area of southern interior British Columbia. This area contains several forest types, from low elevation dry ponderosa pine forests, through Douglas-fir and lodgepole pine forests, to montane spruce forests, to the high elevation Engelmann spruce/subalpine fir forests.

The experimental design was as follows (Figure 1): For each subzone, three plots were established, with 30 to 40 trees per plot depending on the site. The species that were selected are hybrid spruce (Sx), lodgepole pine (*Pinus contorta*, Pl) and Douglas-fir (Pseudotsuga menziesii, Fd). These are the dominant species in this region. More than one species was used per subzone because different species have different insect and pathogen problems. For example, Douglas-fir is a climate sensitive species, but in this region, Douglas-fir experiences spruce budworm outbreaks and tussock moth attacks, and Douglas-fir beetle, the effects of which sometimes mask the tree ring climate signal. Using several species that have different pests or pathogens reduces the confounding of climate effects by mortality agents.

The dominant tree species in ESSFdc are Sx and Pl; Sx, Pl and Fd dominate the MSdm2, while only Fd and Pl are dominant in IDFdk2. Since the idea was to use spatial climatic variation as a comparison with temporal climatic variation, the species sampled need to occur in at least two subzones. This is why all three species were included in the study. Sampling targeted "healthy" (no visible stem decay, no insect attack) and mature trees (at least 80 to 100 years old). For each tree, diameter at breast height (DBH), height, location (longitude, latitude, elevation and aspect) and growth condition (dominant or

subdominant, healthy or diseased, open or closure stand, etc.) and ground vegetation percentage cover were recorded. One core was taken from breast height of each sample tree.

Once the samples were brought back to the laboratory, tree rings were dated and measured for early and late ring width and density by X-ray densitometer. COFECHA (Holmes, 1983, Grissino-Mayer, 2001) is being used to cross date the cores and to make sure there are no errors in dating the cores. COFECHA software examines for false rings or dating errors. Once all the dating is done, ARSTAN (developed by Dr. Edward R. Cook at the Tree-Ring Laboratory, Lamont-Doherty Earth Observatory of Columbia University, Palisades, New York) will be used to de-trend the effects caused by age and competition. Then, the "cleaned" data will be used to construct the relationships of ring width and density to climatic factors. The future tree growth will then be predicted based on climatis data. The samples from MSdm2 will be used to compare actual real ring width with simulated ring width using FORECAST. The data from ESSFdc and IDFdk2 will then be combined with the MSdm2 data to evaluate the performance of FORECAST along the elevational climatic gradient. This will include predicting variation of the growth from the MS under the climate regimes of ESSF and IDF as a test of elevation sequences as an analogue of temporal sequences.

5 Conclusions

5.1 Summary of key findings

An approach to the prediction of the spatial and temporal variations in climatic favourability for MPB was developed by combining a model for interpolating daily precipitation and air temperature data in areas of complex terrain with favourability indices adapted from those used by Safranyik et al. (1975) and Carroll et al. (2004), which were based on climate normals. A key difference between the normal-based indices and those employed in this study was the use of a seasonally varying threshold for cold mortality. When applied to the Chilcotin outbreak in the 1970s and 1980s, the approach revealed statistically significant skill in identifying cell-years that were climatically favourable and thus had a higher probability of increased infestation. However, increased infestation was frequently observed in cells that were predicted to be climatically unfavourable. Possible sources of prediction error include (1) errors in the interpolated weather observations, (2) occurrence of favourable microclimatic settings (e.g., warm, south-facing aspects, areas of deep snow that would insulate the lower portions of tree trunks from severe cold) even in areas with unfavourable macroclimatic conditions, (3) uncertainty in the threshold values used in the indices and (4) effects of MPB population dynamics (e.g., density-dependent processes).

The approach was also applied to three transects crossing the Rocky Mountains in the vicinities of Banff, Jasper and Pine Pass. Observed outbreak patterns for all three transects were broadly consistent with the computed favourability indices. Winter cold mortality appeared to be the most frequent limiting factor for MPB expansion. However, annual heat accumulation was also frequently below the threshold for favourability at the highest points on the Banff transect (Kicking Horse Pass, Lake Louise, Bow Valley). The years 1999 to 2001 were dominantly favourable at all sites, and this sequence of favourable years likely provided the conditions required for establishment of MPB on the east side of the Rockies.

The time series of the climatic favourability indices suggest that winter cold mortality played a dominant role in controlling MPB spread through the period since 1948 and up to the current outbreak. For example, the Chilcotin outbreak appears to have ended abruptly as a result of early cold snaps in the autumns of both 1984 and 1985. To examine the climatology of cold mortality events, synoptic circulation patterns based on daily grids of mean sea-level-pressure (MSLP) were classified into 13 types using a standard pattern-recognition technique. It was found that the circulation type representing Arctic outbreak conditions had the most frequent association with potential cold-mortality events throughout the province, though other types played a role in northern British Columbia.

There did not appear to be simple trends in synoptic-type frequencies. However, the interannual variations in the frequencies were significantly associated with different phases of large-scale ocean-atmosphere teleconnections, including El Niño-Southern Oscillation (ENSO), Pacific North America pattern (PNA) and the Pacific Decadal Oscillation (PDO). In particular, the frequencies of the synoptic types associated with potential cold-mortality events were lower in the neutral and positive phases of PDO, which have dominated since the occurrence of a major regime shift in 1976-1977. Furthermore, the conditional probability of having a day with temperatures below the cold-mortality threshold, given the occurrence of a "cold" synoptic type, was lower in neutral and positive phases of PDO. Therefore, the net effect was that the dominance of neutral and positive phases of PDO since 1977 has been associated with less frequent and less severe cold spells and hence greater favourability for MPB expansion. The climate changes associated with the PDO shift therefore appear to provide a reasonable proximal explanation for the more favourable winter climate. However, it is possible that the PDO shift is, itself, only one manifestation of a larger-scale climate phenomenon.

5.2   Implications for future expansion of Mountain Pine Beetle

There did not appear to be any climate-change scenarios readily available that provided daily output, thus limiting the application of the favourability indices developed in this study for the examination of the potential for future spread. However, the association between decreased winter cold mortality and the dominance of neutral and positive phases of PDO suggests that, unless there is a shift back to dominance by the negative phase of PDO (which was the case prior to about 1922 and between about 1947 and 1976), winter climatic conditions are unlikely to limit the spread of MPB throughout central British Columbia. The situation for the northeast of the province is less clear based on historic trends, although they do suggest an increased frequency of favourable winter conditions in recent years.

An initial goal of this study was to examine the coupled effects of climate and stand conditions. This goal was not completely addressed within the time frame of the study, but should be possible once the climate-FORECAST modelling scheme has been developed further.

5.3   Suggestions for further research

It appears that MPB spread through central and southern British Columbia is currently well established and will not be subject to climatic limitations if current large-scale conditions and trends prevail through

the future. In addition, MPB have spread across the Rockies, so the role of the mountain passes as climatic barriers is no longer a valid consideration. Further research should focus on conditions in Alberta and the northeast of British Columbia to assess recent trends in climatic favourability and the potential for further spread of MPB across the boreal forest into eastern North America.

In terms of the climatic favourability indices, further research is needed on MPB biology and population dynamics to define more precisely the climatic thresholds for expansion. Further research is also needed to improve the calculation of the indices. In particular, improved methods are required for interpolation of minimum daily air temperature from existing weather data, particularly in areas with complex topography. Approaches are required that can account for effects of cold air drainage and ponding during the extreme conditions that can cause mortality, and should account for the prevailing synoptic conditions and the topographic settings of the weather stations. In addition, approaches are required for predicting the effects of microclimatic variability on temperatures within the bark.

Further studies should address the role of population dynamics, particularly the role of density-dependent processes, and how these interact with climatic conditions and stand-level attributes. A recent survey of sites west of Prince George found infestations in 20-year-old stands (Vaughn Palmer, *Vancouver Sun*, page A3, 15 June 2005), not just the mature stands (typically 80 to 160-year-old) previously thought to be vulnerable. The longer term significance for re-establishment of pine stands under favourable climatic conditions is an important question.

6 References

Alberta Government. 2005. http://www3.gov.ab.ca/srd/forests/health/mpb.html. [last accessed 6 Apr 2005]

Bitz, C.M. and Batisti, D.S. 1999. Interannual to decadal variability in climate and glacier mass balance in Washington, western Canada and Alaska. Journal of Climate 12:3181-3196.

Bolstad, P.V., Swift, L., Collins, F. and Régnière, J. 1998. Measured and predicted air temperatures at basin to regional scales in the southern Appalachian mountains. Agricultural and Forest Meteorology 91:161-178.

Carroll, A.L., Taylor, S.W. and Régnière, J. 2004. Effects of Climate Change on Range Expansion by The Mountain Pine Beetle in British Columbia. Final contract report prepared for the British Columbia Ministry of Water, Land and Air Protection.

Dahni, R.R. 2004. Synoptic Typer Reference Manual Version 2.2. February 2004. Commonwealth Bureau of Meteorology.

Dahni, R.R. and Ebert, E.E. 1998. Automated objective synoptic typing to characterize errors in NWP model QPFs, J31-J34, 12th Conference on Numerical Weather Prediction, Phoenix, Arizona, 11-16/1/98.

Grissino-Mayer, H. D. 2001. Evaluating crossdating accuracy: a manual and tutorial for the computer program COFECHA. Tree-ring Research 57: 205-221.

Hasenauer, H., Merganicova, K., Petritsch, R. Pietsch, S.A. and Thornton, P.E. 2003. Validation of daily climate interpolations over complex terrain in Austria. Agricultural and Forest Meteorology 119:87-107.

Holdaway, M.R. 1996. Spatial modeling and interpolation of monthly temperature using kriging. Climate Research 6: 215-225.

Holmes, R. L. 1983. Computer-Assisted quality control in tree ring dating and measurement. Tree-Ring Bulletin. 43: 69-78.

Kimmins, J.P., Mailly, D. and Seely, B. 1999. Modelling forest ecosystem net primary production: the hybrid simulation approach used in FORECAST. Ecological Modeling 122:195-224.

Logan J.A. and Powell, J.A. 2001. Ghost forests, global warming, and the mountain pine beetle (Coleoptera: Scolytidae). American Entomologist 47:160-173.

Mantua, N.J., Hare, S.R., Zhang, Y., Wallace, J.M. and Francis, R.C. 1997. A Pacific interdecadal climate oscillation with impact on salmon production. Bulletin of the American Meteorological Society 78:1-11.

Moore, R.D. and Demuth, M.N. 2001. Mass balance and streamflow variability at Place Glacier, canada, in relation to recent climate fluctuations. Hydrological Processes 15:3473-3486

Moore, R.D. and McKendry, I.G. 1996. Spring snowpack anomaly patterns and winter climatic variability, British Columbia, Canada. Water Resources Research 32:623-632

Nalder, I.A. and Wein, R.W. 1998 Spatial interpolation of climatic normals: test of a new method in the Canadian boreal forest. Agricultural and Forest Meteorology 92:211-225.

Redmond, K.T. 2005. http://www.wrcc.dri.edu/enso/ensodef.html. [last accessed 31 March 2005]

Redmond, K.T. and Koch R.W. 1991. Surface climate and streamflow variability in the western United States and their relationship to large-scale circulation indices. Water Resources Research 27:2381-2399.

Running, S.W., Nemani, R.R. and Hungerford, R.D. 1987. Extrapolation of synoptic meteorological data in mountainous terrain and its use for simulating forest evapotranspiration and photosynthesis. Canadian Journal of Forest Research 17:472-483.

Safranyik, L., Shrimpton, D.M. and Whitney, H.S. 1975. An interpretation of the interaction between lodgepole pine, the mountain pine beetle and its associated blue stain fungi in western Canada. In: D.M. Baumgartner (ed), Management of Lodgepole Pine Ecosystems. Washington State Univ. Coop. Ext. Serv., Pullman, WA. pp. 406- 428.

Seely, B., Nelson, J., Wells, R. Peter, B., Meitner, M., Anderson, A, Harshaw, H., Sheppard, S., Bunnell, F., Kimmins, H. and Harrison, D. 2004. The application of a hierarchical, decision-support system to evaluate multi-objective forest management strategies: A case study in northeastern British Columbia, Canada. Forest Ecology and Management 199: 283–305.

Seely, B., Arp, P. and Kimmins, J. P. 1997. A forest hydrology submodel for simulating the effect of management and climate change on stand water stress. Presented at a conference on "Empirical and process-based models for forest tree and stand growth simulation," 21-27 September 97, Oeiras, Portugal.

Shabbar, A. and Bonsal, B. 2004. Associations between low frequency variability modes and winter temperature extremes in Canada. Atmosphere-Ocean 42:127-140.

Shabbar, A., Bonsal, B. and Khandekar, M. 1997. Canadian precipitation patterns associated with the southern oscillation. Journal of Climate 10:3016-3027.

Taylor, S.W. and Erickson, R.D. 2003. Historical mountain pine beetle activity. http://www.pfc.cfs.nrcan.gc.ca/entomology/mpb/historical/index_e.html

Thompson, D.W.J. and Wallace, J.M. 1998. The Arctic Oscillation signature in the wintertime geopotential height and temperature fields. Geophysical Research Letters 25:1297-1300.

Thornton, P.E., Running, S.W. and White, M.A. 1997. Generating surfaces of daily meteorological variables over large regions of complex terrain. Journal of Hydrology 190:214-251.

Trenberth, K.E. 1990. Recent observed interdecadal climate changes in the Northern Hemisphere. Bulletin of the American Meteorological Society 71:988-993.

Wallace, J.M. and Gutzler, D.S. 1981. Teleconnections in the geopotential height field during the northern hemisphere winter. Monthly Weather Review 109:784-812.

Wallace, J.M. and Thompson, D.W.J. 2002. Annular modes and climate prediction. Physics Today 55:28-33.

Wygant, N.D. 1937. Effects of low temperatures on the Black Hills Beetle (Dendroctonus Ponderosae Hopk.). Doctoral Thesis. New York State College of Forestry.

Yarnal, B. 1993. Synoptic Climatology in Environmental Analysis: A Primer. Belhaven Press. London. Kimmins, J.P., D. Mailly and B. Seely. 1999. Modelling forest ecosystem net primary production: the hybrid simulation approach used in FORECAST. Ecological Modeling 122:195-224.